MDOT RC-1454
CSD-2004-06

MDOT

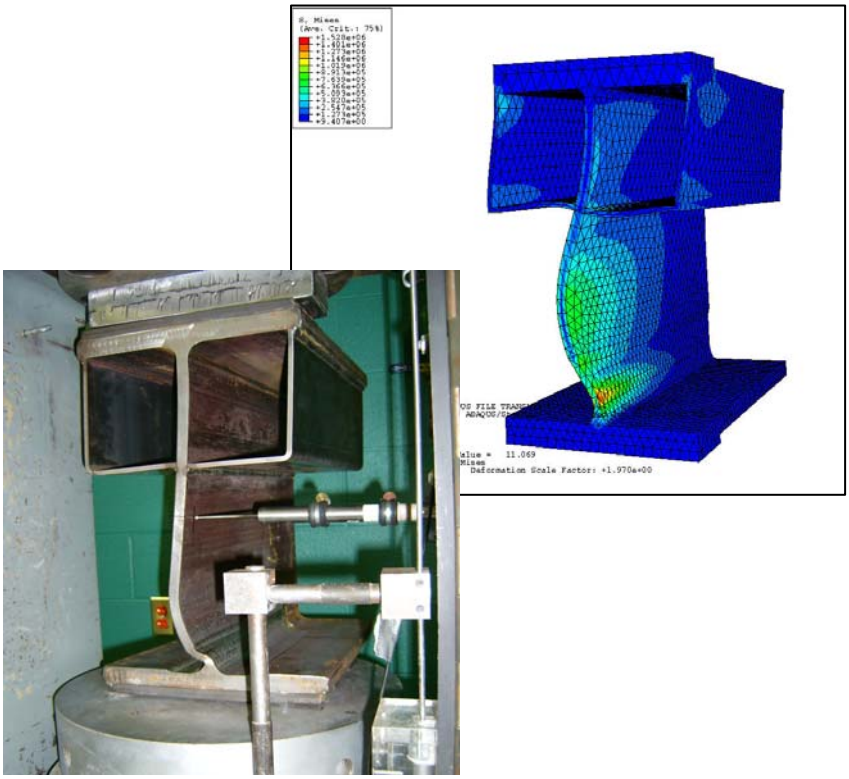

Research

DEVELOPMENT OF STEEL BEAM END DETERIORATION GUIDELINES

FINAL REPORT – JANUARY 2005

MichiganTech

CENTER FOR STRUCTURAL DURABILITY
MICHIGAN TECH TRANSPORTATION INSTITUTE

Technical Report Documentation Page

1. Report No. Research Report RC-1454	2. Government Accession No.	3. MDOT Project Manager Robert Kelley, P.E.
4. Title and Subtitle Development of Steel Beam End Deterioration Guidelines		5. Report Date January 5, 2005
7. Author(s) John W. van de Lindt and Theresa M. Ahlborn		6. Performing Organization Code MTU
9. Performing Organization Name and Address Michigan Technological University 1400 Towsend Drive Houghton, MI 49931-1295		8. Performing Org Report No. CSD-2004-06
12. Sponsoring Agency Name and Address Michigan Department of Transportation Construction and Technology Division P.O. Box 30049 Lansing, MI 48909		10. Work Unit No. 11. Contract Number: MITRA0010 11(a). Authorization Number:
15. Supplementary Notes .		13. Type of Report & Period Covered Final Report, 2003-2004 14. Sponsoring Agency Code

16. Abstract

Corrosion of steel bridge beams due to deicing media is a very common problem in northern regions of the U.S. The deterioration of steel beam ends due to deck joint leakage and occasional spray from passing vehicles usually consists of irregularly shaped holes, termed section losses, which typically occur in the web near or directly above the bearing area. This may result in decreased shear capacity, web crippling, or web buckling. This report presents the results of a study sponsored by the Michigan Department of Transportation whose purpose was to provide the structural analyst with simplified methods for computing the reduced capacity of the section, i.e. determination of whether or not a bridge should be posted for trucks. The guidelines are based on the results of finite element analyses (FEA) for a suite of sixteen typical steel girder bridges.

The most common shapes and locations for steel beam end deterioration were identified by reviewing detailed inspection reports for various bridges in order to develop a simulation matrix of corrosively damaged steel beams for finite element analysis. Bridge plans and inspection reports were used to identify the needed beam and slab dimensions as well. Analyses of the steel beam ends with simulated damage of various sizes and shapes were performed by using finite element software SDRC IDEAS and ABAQUS. Experimental work was performed on a selected beam to verify the validity of finite element analysis. Design charts were developed for various cases of damage based on FEA results. The structural analysis guidelines consist of factors used to estimate the reduced load capacity of the deteriorated steel beam from existing AISC capacity equations.

17. Key Words: Steel, deterioration, beam end, buckling.	18. Distribution Statement No restrictions. This document is available to the public through the Michigan Department of Transportation.		
19. Security Classification (report) Unclassified	20. Security Classification (Page) Unclassified	21. No of Pages 60	22. Price

Development of Steel Beam End Deterioration Guidelines

Submitted by:

John W. van de Lindt & Theresa M. Ahlborn

Final Report – January, 2005

Michigan Tech Transportation Institute
Center for Structural Durability
MDOT Research Report RC-1454
CSD-2004-06

ACKNOWLEDGEMENTS

This project was financially supported by the Michigan Department of Transportation in cooperation with the Federal Highway Administration. The authors would like to thank the members of the Michigan Department of Transportation (MDOT) Research Advisory Panel (RAP) for their guidance and suggestions throughout the course of the project.

DISCLAIMER

The content of this report reflects the views of the authors, who are responsible for the facts and accuracy of the information presented herein. This document is disseminated under the sponsorship of the Michigan Department of Transportation in the interest of information exchange. The Michigan Department of Transportation assumes no liability for the content of this report or its use thereof.

TABLE OF CONTENTS

LIST OF FIGURES

Figure **page**

LIST OF TABLES

Table **page**

1. INTRODUCTION

1.1 Research problem and background

According to the 2003 Michigan state bridge inventory, 40% of state-owned bridges built in the last decade are steel girder bridges. This number is even greater if one considers all the existing bridges in the state. Corrosion of steel beams primarily due to deicing media made of salt and water is a very common problem in the state of Michigan. This generally takes the form of localized deterioration of steel beam ends usually from deck joint leakage and occasional spray from passing vehicles. The deterioration usually consists of thinning sections in the web or irregularly shaped holes in the web just above the flange and may decrease the load carrying capacity in shear, bearing, and sometimes bending. The web in bearing and shear has been shown to be the governing failure mode when analyzing capacity loss due to end corrosion in steel girders (Kelley, 2004). Particularly, localized buckling and crushing at the base of the web has been observed by Michigan Department of Transportation (MDOT) bridge inspectors and/or engineers.

Reduced capacity sections are generally handled on a case-by-case basis by MDOT and often require a more detailed analysis than straight forward design equations, i.e. finite element analysis. The simplified method used by MDOT often does not consider a portion of the remaining steel, leading to results that may be too conservative and then to more costly repairs and replacement of beams which may not be necessary.

Presently guidelines for MDOT personnel to determine when section loss of web or flange deterioration is critical and should be reported to a structural analyst for further analysis are limited and very subjective. Further, there is no accepted standard to determine the reduced load carrying capacity for the structural analyst. This report focuses on the development of guidelines to assist the structural analysts in accurately determining the remaining capacity of the beam, quickly and accurately without numerical analysis.

Figure 1.1 shows an example of typical deterioration on a bridge beam (excerpted from NCHRP 333, 1990). Notice that there are three types of corrosion in a typical steel beam namely crevice corrosion, deposit attack, and uniform corrosion. Crevice corrosion will not be considered in this report; only the two latter types of corrosion will be considered.

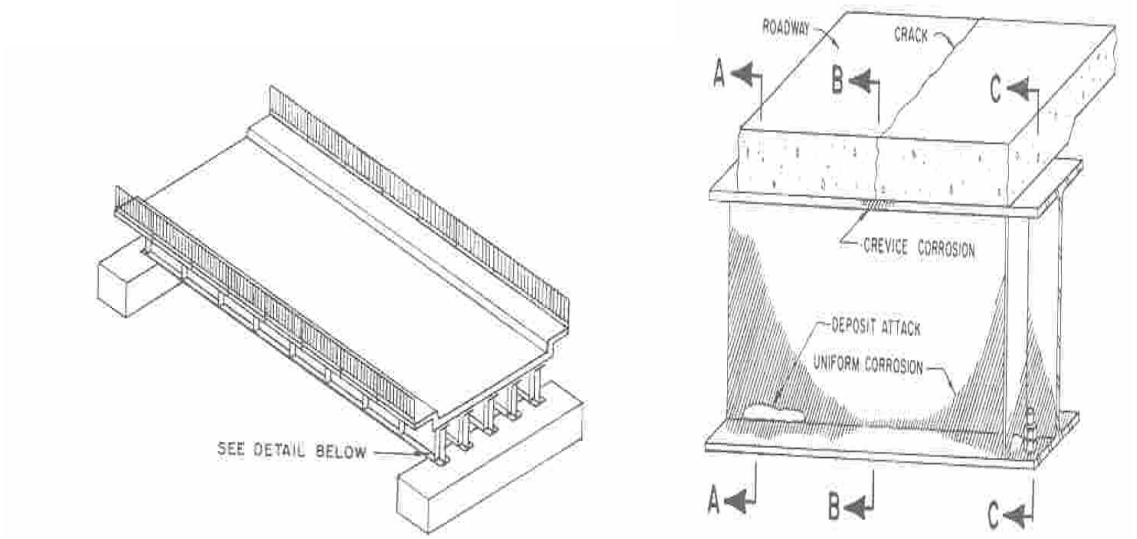

Figure 1.1 Composite beam showing corrosion at the steel beam end (NCHRP 333, 1990)

Figure 1.2 and Figure 1.3 shows the typical pattern of corrosion commonly observed near steel beam ends by the MDOT bridge inspectors. This type of corrosion leads to the thinning of the bottom portion of the web as well as bottom flange thickness reduction and can result in a significant reduction in capacity.

Figure 1.2 Deterioration near steel beam end (photo taken by MDOT bridge inspector)

Figure 1.3 Deterioration near steel beam end (photo taken by MDOT bridge inspector)

1.2 Research objectives

The scope of this study was limited to rolled steel sections most commonly used by MDOT. The immediate research objectives of this study are:

1. To identify the common types of damage in steel beam ends and determine which areas of damage in a section are most critical.
2. Using the results of (1), develop a model that can provide structural analysts with a simplified approach for computing the reduced capacity of typical bridge sections.

These objectives were accomplished through several tasks, including a series of three-dimensional Finite Element Analyses (FEA) that were used to determine the reduced capacities for common deterioration types against several different possible failure mechanisms. Verification of the numerical analysis through experimental testing was also completed within the scope of this study and will be addressed later.

1.3 Summary of existing information

NCHRP Report 333 (Kulicki et. al. 1990) outlines field inspection guidelines, different forms of corrosion for steel bridges such as uniform corrosion, localized corrosion, deposit attack, and pitting, types and techniques of corrosion inspection, and condition rating of bridges based on the corrosion level. It also includes the evaluation process for the load carrying capacity of a bridge and the elements affected by corrosion which includes (1) selection of evaluation method, (2) evaluating the strength of the bridge members, (3) defining the type of loads to be used, (4) calculating the resulting member loads and (5) defining the required safety levels.

The evaluation procedure for corrosion effects on bridges has three phases. Phase 1 includes collecting bridge data, understanding the structure behavior and coordinating the purpose of inspection with the bridge inspector. Phase 2 identifies the criticality of the conditions created by corrosion and urgency of required actions. It includes examining

the inspection report and addressing the location of damage, nature of damage, amount and geometry of damage, extent of damage and environment conditions. Phase 3 includes quantitative evaluation, which determines the residual capacity of a deteriorated bridge.

The quantification of corrosive damage is necessary to calculate the reduced capacity. NCHRP 333 defines the parameters; percentage section loss, loss coefficient, length of loss, and transition from reduced to full section in order to quantify the corrosion damage. Percentage section loss (*%loss*) is defined as the amount of metal loss at a given location on a bridge member,

$$\%loss = (1 - \frac{A_d}{A_o})100 \tag{1.1}$$

where A_o is the original cross sectional area and A_d is the reduced cross sectional area.

Loss coefficient (q) is the amount of metal loss at a given location along a member. It is defined as,

$$q = \frac{A_o}{A_d} = \frac{100}{100 - \%loss} \tag{1.2}$$

Length of loss is the extent of loss along a member. The transition from reduced to full section can be abrupt or gradual depending on the corrosion type. The damage effects at the local level are quantified by using a *local residual capacity factor, RCF_l* defined as:

$$RCF_l = \frac{100 - \%loss}{100} = \frac{1}{q} \tag{1.3}$$

The damage effects at the member level are quantified by using a *member residual capacity factor*, RCF_m defined as:

$$RCF_m = \frac{C_{dm}}{C_m} \tag{1.4}$$

where C_m is the capacity of the original member and C_{dm} is the capacity of the damaged member.

NCHRP 333 considers the load carrying capacity of a rolled shape member by its resistance to overall or local buckling. Corrosion forms such as uniform corrosion can

reduce the section area and other section properties like moment of inertia and radius of gyration, thus affecting the stability of the member. Overall failure of a steel beam may result from web buckling, compression yielding, or a combination of both. Uniform corrosion can increase the width-thickness ratio, *b/t*, and result in localized buckling of the steel beam.

Nowak and Kayser (1989) developed a corrosion damage model for simple-span steel girder bridges. This paper defines five common forms of corrosion which can affect a steel girder bridge namely (1) general corrosion, (2) pitting corrosion, (3) galvanic corrosion, (4) crevice corrosion and (5) stress corrosion. The corrosion loss follows an exponential function

$$C = a \times n^b \tag{1.5}$$

where C is the average corrosion penetration in microns, n is the number of years and a and b are the parameters determined from regression analysis of experimental data. A reduction in section area will decrease the geometric properties and buckling capacity of members can be critically affected by the reduction in metal thickness. The amount of capacity reduction caused by loss of section depends whether the component is in compression or tension. The corrosion in a steel girder may affect the capacity in bending, shear, and bearing (buckling, crippling, and crushing). Three failure modes of bending are yielding of steel, crushing of concrete or slippage in the composite connectors of which steel yielding is preferred to allow ductile failure. Nowak and Kayser (1989) developed an analytical model for bending was developed to evaluate bending behavior of composite sections. The loss in web material will reduce the shear capacity due to section loss and web buckling. The three analysis methods used for evaluating the web bearing strength were the effective-width method, plastic hinge failure mechanism, and plate theory. Plate theory was used to evaluate the bearing capacity of the web. This bearing model accounted for the web buckling. It was shown that buckling of the web is the critical mode of failure for a short span bridge. This was also observed in the present study as well as by MDOT analysts.

1.4 Selection of bridge portfolio

A bridge portfolio of sixteen simply-supported rolled beam bridges was selected from the 2003 MDOT bridge inventory. Bridges were selected that were built between 1950 and 1990 with the objective of performing finite element analyses. Isolated beams were selected for analysis as it is conservative. The portfolio approach was selected since it was impossible to analyze every bridge beam under all conditions. The following table shows the details of the bridges selected for this study.

Table 1.1 Bridge portfolio selected for finite element analyses

No	Structure_id	Girder Type	Span Length [ft]	Girder Spacing[ft]	Composite section	Slab Thickness[in]	Year built
1	S02-110534	W 36X230	78	4.6	yes	7	1952
2	S05-58033	W 36x260	82.3	5.3	yes	9	1950
3	S12-82191	W 36x150	82	10	yes	9	1966
4	S16-13073	W 36x 194	82	7.5	yes	7.5	1968
5	S14-25032	W 33x152	72.6	4	yes	8.25	1958
6	S12-77111	W 33x141	70	5.66	yes	9	1965
7	S09-25032	W 33x141	70.3	4.5	yes	8	1957
8	B01-58034	W 33x130	47	6	yes	9	1958
9	B01-20015	W 33x130	68.75	5	yes	9	1960
10	S04-20015	W 33x130	47	4.57	yes	7	1961
11	S30-82112	W 30x116	55	5.83	yes	7	1963
12	S06-47064	W 30x108	57	5.33	yes	7	1962
13	B01-42021	W 27x84	48.75	7.3	yes	9	1988
14	S14-82024	W 33x130	54	4.5	yes	7	1955
15	S10-82252	W 36x150	60	8	yes	9	1969
16	S50-82123	W 36x170	86	7	yes	10	1972

2. NUMERICAL ANALYSIS

2.1 Introduction

In order to meet the research objectives outlined in Section 1.2, the bridge beams in the bridge portfolio (see Section 1.4) were analyzed in order to determine their buckling capacity. This was accomplished by modeling a short section of each beam within the bridge portfolio with varying levels and shapes of artificially induced damage. Damage was modeled simply by removing a section of the beam that was deteriorated, since those sections have zero capacity. A numerical crushing/buckling analysis was then performed to determine the remaining capacity.

2.2 Finite element model

The finite element model used in the analyses consists of a beam section three feet in length with a bearing length of 5 inches. Figure 2.1 shows the I-DEAS model of a W30x108 beam. The mesh which was auto-generated in IDEAS, is shown in Figure 2.2.

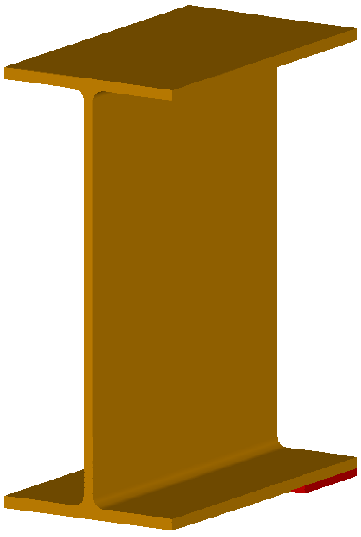

Figure 2.1 I-DEAS model of W30x108 beam used for buckling/crushing analysis

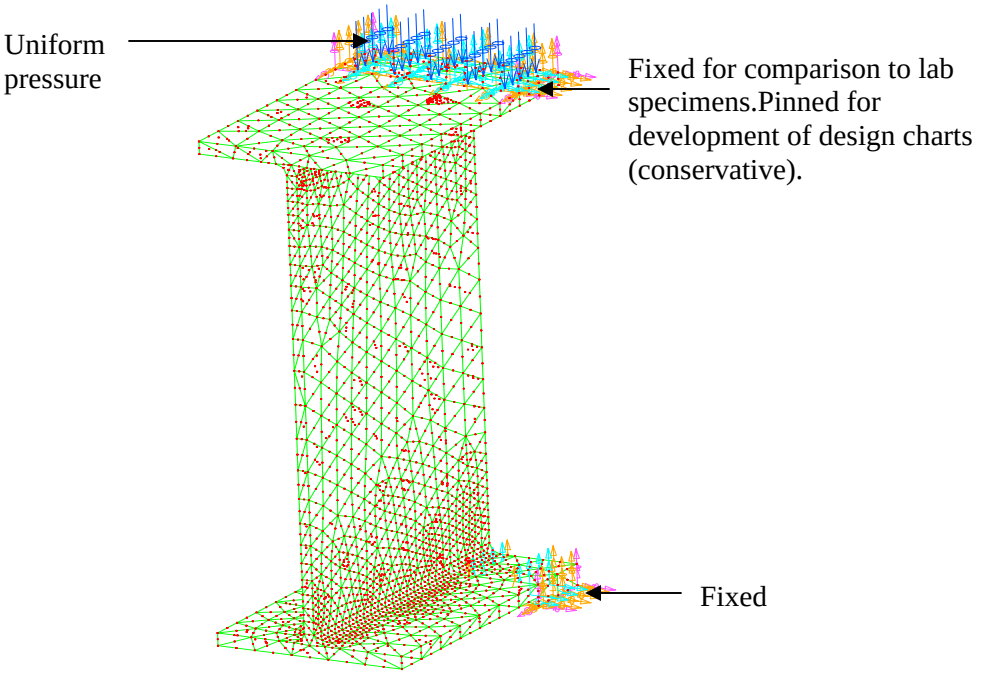

Figure 2.2 IDEAS mesh and boundary conditions used for the W30x108 model

2.3 Finite element analysis procedure

The Buckling/Crushing load was estimated by using the finite element analysis software SDRC I-DEAS and ABAQUS in succession. SDRC I-DEAS was used as a preprocessor to generate the mesh for the beam model. The input file was then exported to ABAQUS and solved numerically using the ABAQUS numerical solver. The procedure is shown using “print screen” capability in Appendix B. Solid parabolic tetrahedral elements with 10 nodes and 6 degrees of freedom at each node were used for meshing. The solid tetrahedral elements are used in order to account for the complexity of the model and their ability to integrate well with 3-D models. The boundary conditions are fixed at the bottom and pinned at top which is consistent with previous analyses of this type. An eigenvalue buckling analysis was performed in order to find the buckling mode shapes. The lowest eigenvalue is the Buckling/Crushing load for a particular beam allows calculation of the buckling capacity.

1.3.1 Theory of buckling

The ABAQUS software uses an incremental solution to the stiffness equation

$$([k_0] + \lambda_i [k_d])\{V_i\} = \{0\}$$

where $[k_o]$ is the initial stiffness matrix, $[k_d]$ is the stiffness matrix due to the incremental loading pattern, λ_i are the eigenvalues, $\{V_i\}$are the buckling mode shapes (eigenvectors) and i refers to the i^{th} buckling mode. The lowest eigenvalue is the governing buckling load. In all the analyses performed, the lowest eigenvalue is considered as the buckling/crushing load for the beam. Figure 2.3 (a) shows the ABAQUS output of the localized buckling of a W30x108 beam. The critical region where the localized buckling occurs is shown in figure 2.3(b).

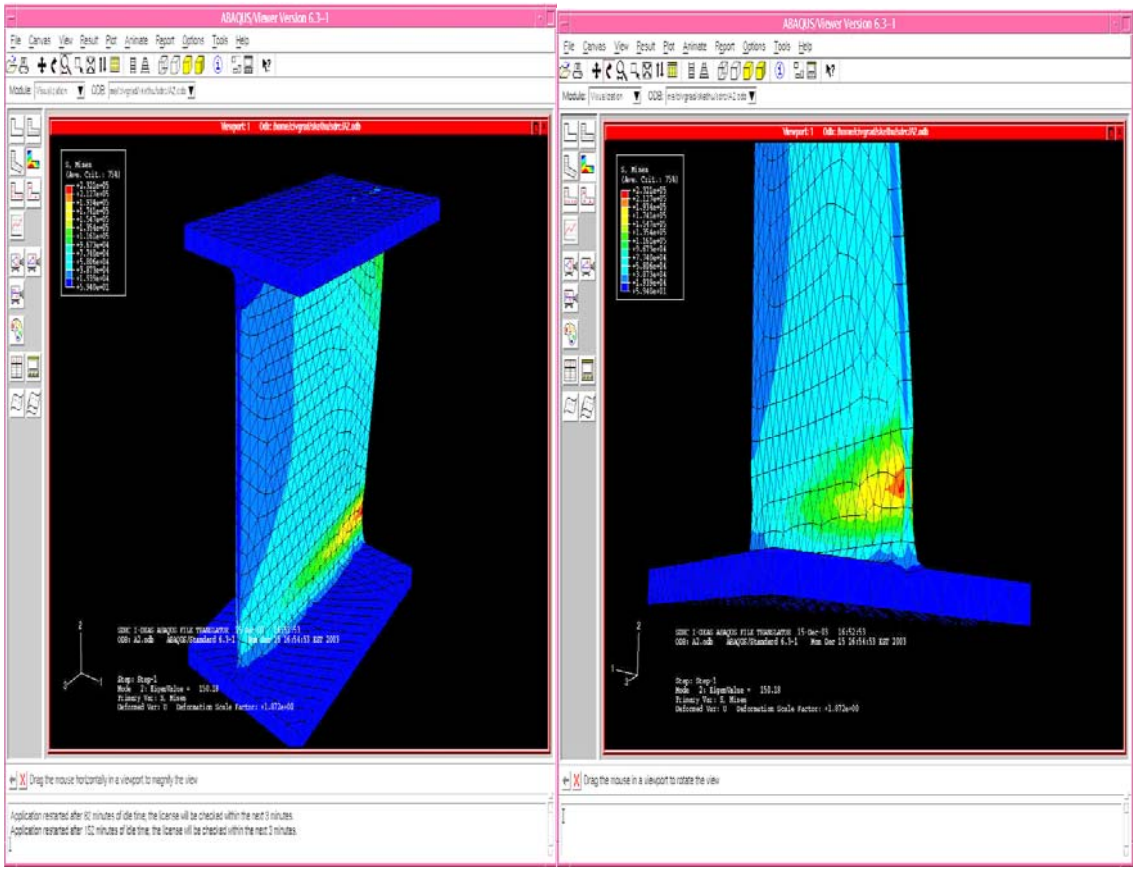

(a) (b)

Figure 2.3(a) and Figure 2.3(b) Localized buckling of the W30x108 beam

It is also possible to do a crushing analysis in ABAQUS, which is simply a displacement extension of the lowest buckling mode.

2.3.2 Crushing analysis

The crushing of a steel beam can also be modeled using the ABAQUS /Explicit crushing analysis. The boundary conditions used for crushing analysis are the same as those used for the buckling analysis. The crushing analysis uses the lowest eigenvalue from the buckling analysis and performs the crushing analysis at the critical region where the lowest buckling value occurs. In the present case the governing mode shape results in crushing at the bottom of the deteriorated web, so the crushing analysis is performed for that critical region. Figure 2.4(a) shows the crushed shape of the W30x108 beam. The critical region where the bottom web of the beam is crushed is shown in Figure 2.4(b).

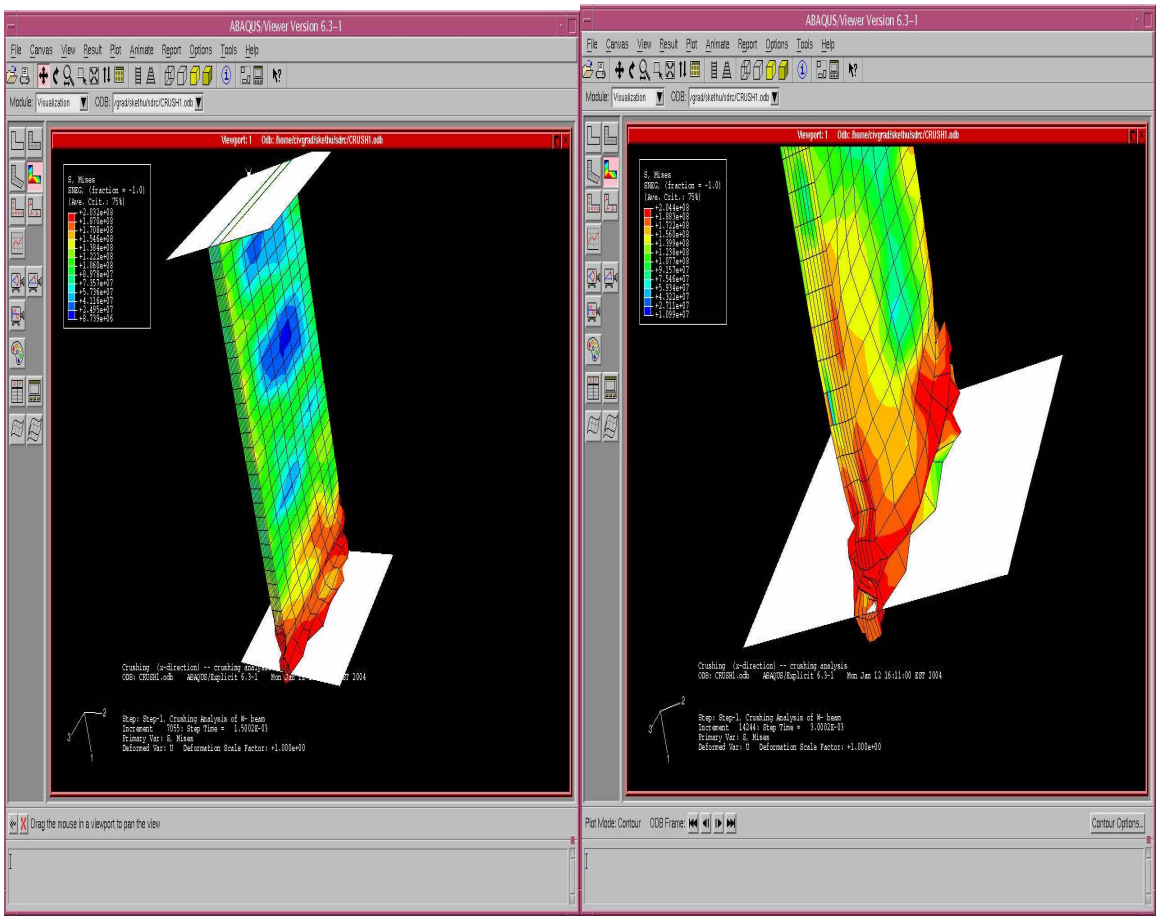

(a) (b)

Figure 2.4(a) and 2.4 (b) Crushing of the W30x108 beam

Recall that the objective of this section was to numerically analyze the remaining capacity of the bridge beam portfolio identified in Section 1.4 under various damage conditions. In order to minimize the number of analyses and simplify the structural analyst guidelines as much as possible a sensitivity analysis was performed for a number of parameters felt to comprehensively describe web and flange deterioration in steel beams. The purpose of the sensitivity analysis was to determine which of these parameters most affected the buckling/crushing capacity of the beams in order to reduce the complexity of the resulting simplified method. In order understand the sensitivity analysis fully, a brief explanation of the terminology used is explained in the following section.

2.4 Terminology used for damage dimensions

The following notation was used for damage dimensions throughout this study.

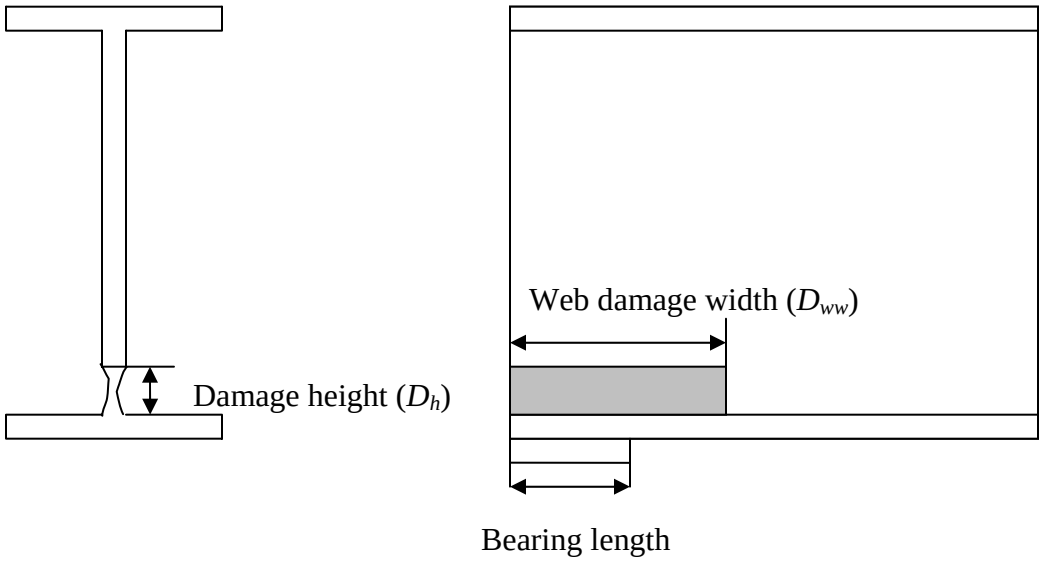

Figure 2.5 Web damage width and damage height for the beam model

A sensitivity analysis on various web damage shapes (triangular, ellipse and rectangular) was performed and it was concluded that the shape of web damage width does not make a significant difference. So, in the present study the rectangular shape was used for simplicity.

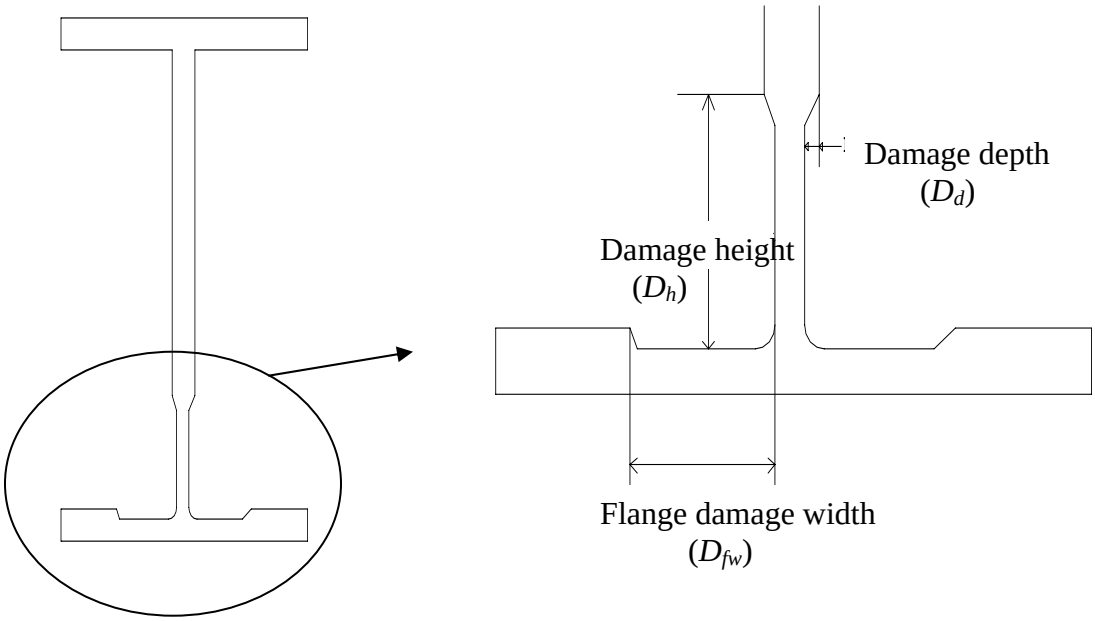

Figure 2.6 Damage height (D_h) and damage depth (D_d) and flange damage width (D_{fw}) for the beam model

Damage depth [D_d]: Thickness of the web lost on one side. It is measured along the thickness of the web. As one would expect it has an influencing effect on the buckling/crushing load.

Damage height [D_h]: Height of web damage. It is measured along the height of the web from the flange (damaged or undamaged). It also has an influencing effect on buckling/crushing load.

Flange damage width [D_{fw}]: Width of damage to the flange. It was determined that it does not affect the buckling/crushing load significantly enough to include in the capacity model.

Web damage width [D_{ww}]: Width of damage along the beam length. It is measured along the span length from the beam end.

2.5 Sensitivity analysis of model parameters

As mentioned, a sensitivity analysis was performed for each of the model parameters just described. Table 2.1 shows the buckling/crushing load values for different flange damage width for a W33x141 beam. Examination of the table shows the insensitivity of beam capacity to the flange damage width for several different damage depths. Based on these results (and others not presented here) it was decided not to use the flange damage width as a parameter I the capacity model.

Table 2.1 Buckling/Crushing loads for different flange damage widths for W30x108

Buckling/Crushing Load [kips]			
Damage depth	**Flange damage width**		
	1.5"	3"	5"
1 / 8"	77	76	76
1/16"	70	69	69

Table 2.2 shows the buckling/crushing load values for different web damage widths for the W33x141 beam. As with the flange damage width, little sensitivity with regards to the buckling/crushing load was observed. Thus this parameter was also eliminated from the model.

Table 2.2 Buckling/Crushing loads for different web damage widths for W33x141

Buckling/Crushing Load [kips]			
Damage depth	**Web damage width**		
	1.5"	3"	5"
1 / 8"	78	78	77
1/16"	72	71	71

Table 2.3 shows the buckling/crushing load values for different web damage widths for a beam. One can see that both these parameters have a significant effect on buckling/crushing load.

Table 2.3 Buckling/Crushing loads for different damage depths and damage heights for W33x141

Buckling/Crushing load [kips]				
Damage depth	**Damage height**			
	0.5”	1.5”	3”	5”
1/16”	77	73	69	64
1/8”	70	60	51	42
3/16”	51	36	30	25

Figure 2.7 shows the graph between capacity remaining versus varying damage depths and damage heights, i.e. the data presented in Table 2.3.

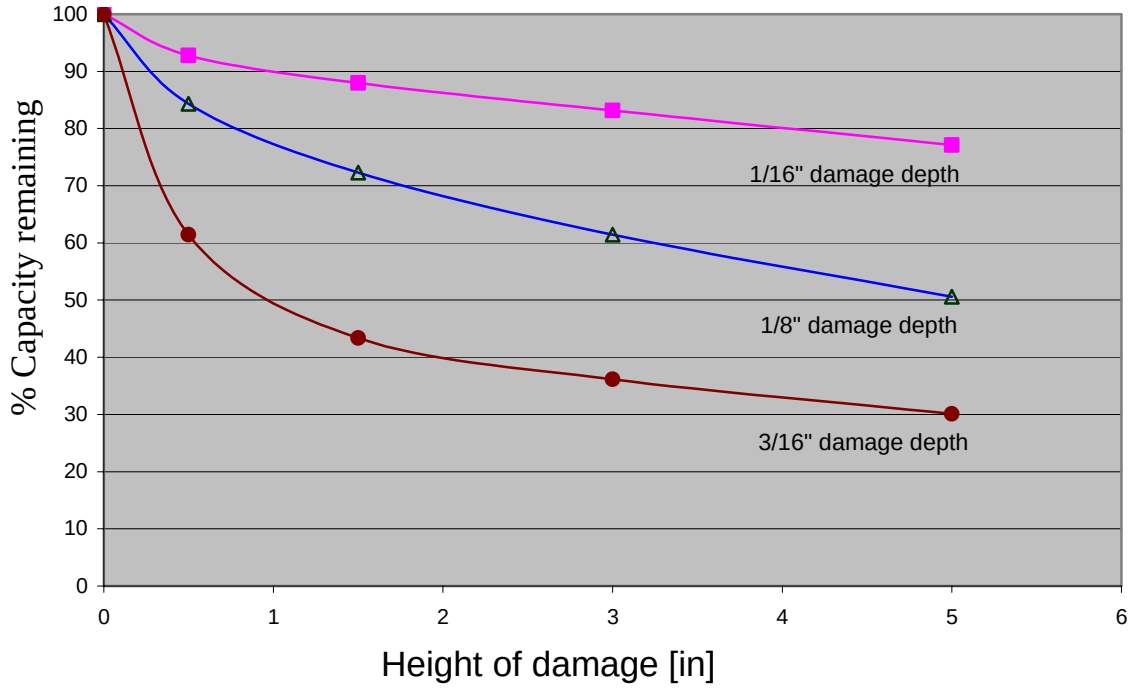

Figure 2.7 Percentage capacity remaining vs damage height for various damage depths

From the above sensitivity analyses it was observed that only damage depth and damage height have a significant effect on the buckling/crushing load. So the remaining analyses for a typical rolled sections and the subsequent model development focused on these two parameters.

3. EXPERIMENTAL PROGRAM

3.1 Introduction

Although the buckling analysis method used in this study is known to be theoretically correct, the accuracy of a perfect numerical solution compared to the imperfect real solution that exists in the laboratory and field was of interest. In other words, experimental verification of the numerical models was the objective of this chapter. A small experimental program was designed that consisted of buckling experiments on four different specimens.

3.1.1 Specimen descriptions

A W18x106 beam was selected for the buckling experiments. Although slightly smaller than most MDOT bridge beams, it was selected for its manageability and was felt to be appropriate for the purposes of this study. Four W18x106 beams with different damage depths and damage heights were tested. Figure 3.1 shows the dimensions of the W18x106 beam tested. Notice that a ¼ inch steel plate was welded to the top flange and upper portion of the web. This was put in place to be representative of a deck or other mechanisms that provide rotational restraint for the upper web of rolled bridge beam sections. Further, this helped force the buckling location to the bottom of the web, where it has typically been observed to occur on existing bridge beams. Figure 3.2 shows a solid model of the W18x106 beam prior to its meshing and export to ABAQUS for numerical analysis of buckling. This is a model of specimen 1 excluding damage to the fillet (discussed later). A 3.5 inch bearing plate was provided at the bottom of the beam. A plate can also be seen at the top of the beam which was simply a spacer plate for loading purposes. Limited lateral bracing at a 7 in. depth was also provided as shown in the figure. This was to force the beam to fail at the bottom. The boundary conditions used for the experiment specimens are fixed at top as well as bottom. The load is applied as a uniform pressure applied on the spacer plate.

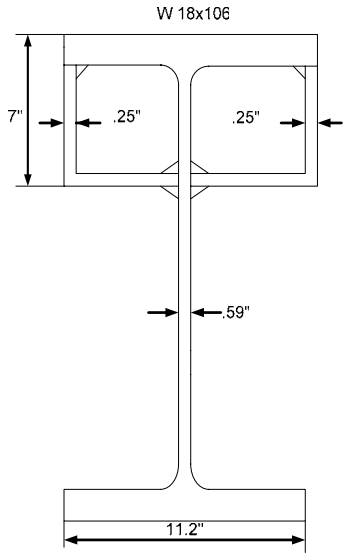

Figure 3.1 Dimensions of W18x106 beam

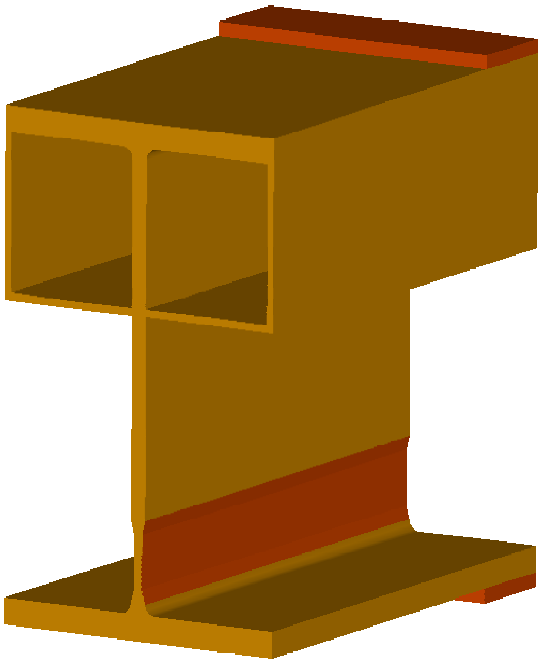

Figure 3.2 SDRC I-DEAS model used for testing

3.1.2 Description of the four test specimens

The four W18x106 beams tested were designated as specimen-1, specimen-2, specimen-3 and specimen-4 based on the order they were tested. Specimen-1 and specimen-2 have damage in the web only whereas specimen-3 and specimen-4 have damage in the web and flange, including the fillet. The latter two were felt to be more representative of field deterioration conditions observed by MDOT personnel, thus their results will be the focus of this chapter.

Specimen-1

This specimen had a web damage height of 3" above the fillet running the entire length of the specimen and a damage depth of 1/8" on each side. The beam was tested using a loading rate of 0.213 in/min. The loading rate was expected to buckle the specimen in approximately two minutes. Figure 3.3 shows the details of specimen-1.

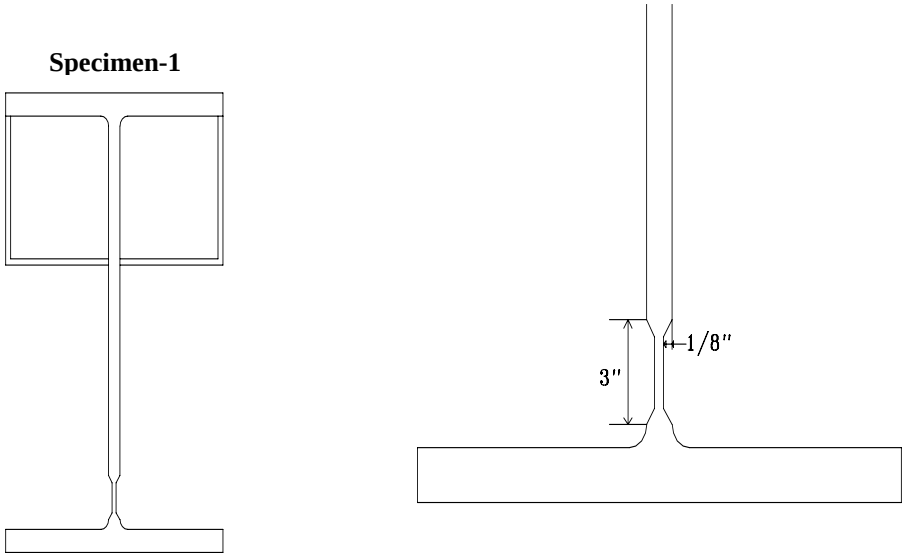

Figure 3.3 Dimensions of specimen-1

Specimen-2

This specimen had a web damage height of 3" above the fillet and a damage depth of 1/16" on each side. This beam was tested using a loading rate of 0.106 in/min. This loading rate

was significantly slower than that of specimen-1. The reason for this slower rate was that specimen-1 buckled too quickly for adequate observation.

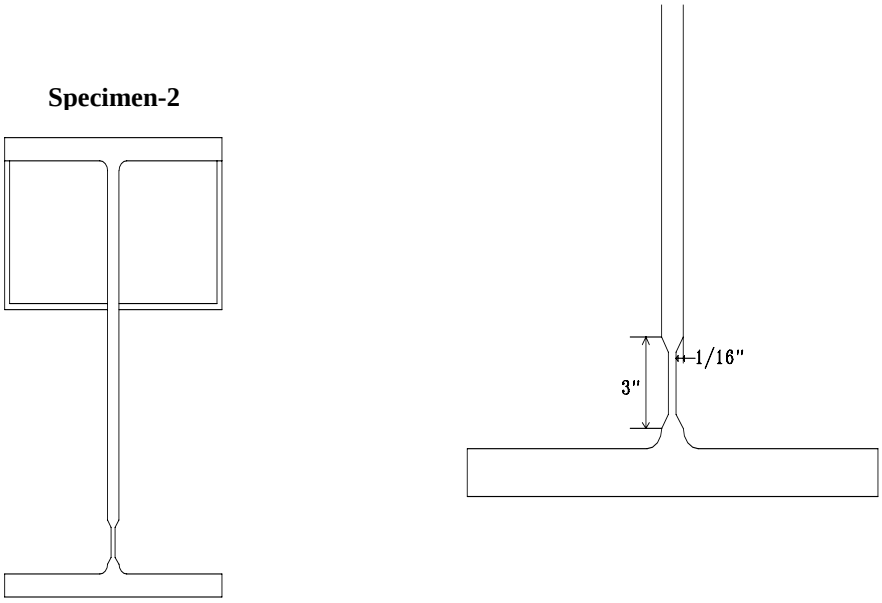

Figure 3.4 Dimensions of specimen-2

Specimen-3

This beam had a web damage height of 1.5”, flange damage width of 1.5”, and a damage depth of 1/8” on each side. This beam was at a loading rate used of 0.106 in/min, and a schematic is presented in Figure 3.5.

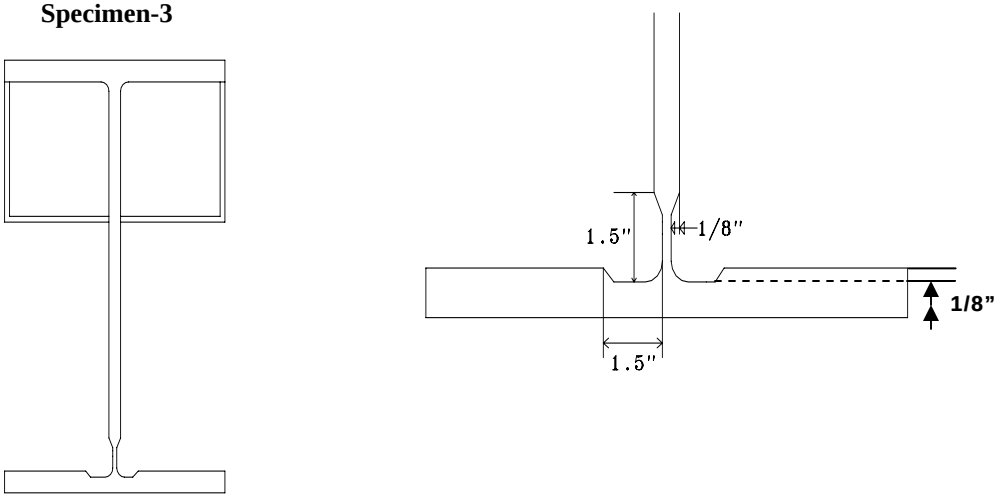

Figure 3.5 Dimensions of specimen-3

Specimen-4:

This beam had a web damage height of 1.5”, flange damage of 1.5”, and a damage depth of 1/16” on each side. This beam was also tested on March 8, 2004. The loading rate used for this beam was 0.106 in/min. A schematic of the specimen is presented in Figure 3.6.

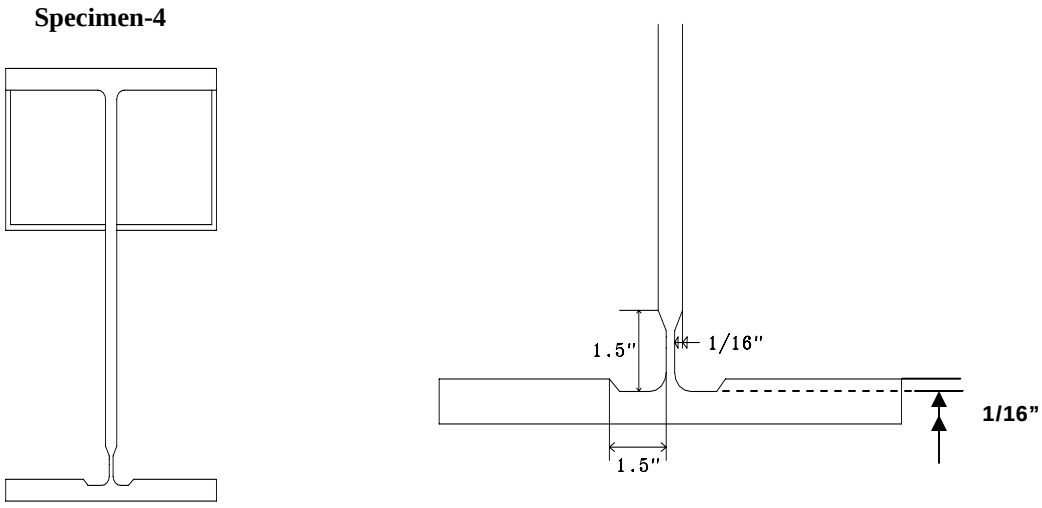

Figure 3.6 Dimensions of specimen-4

3.2 Experimental setup

The specimens were tested in aone million pound MTS test frame with an Instron control system located in the M&M building at Michigan Technological University. Two spring loaded linear variable displacement transducers (LVDTs) were used to measure the lateral displacement of the web. One LVDT was placed at the center of the web damage and the other LVDT was placed at the center of the beam height. Figure 3.7 shows a solid model of the test setup (LVDTS shown on one side for clarity) as well as a photograph of the beam in the test machine just prior to loading.

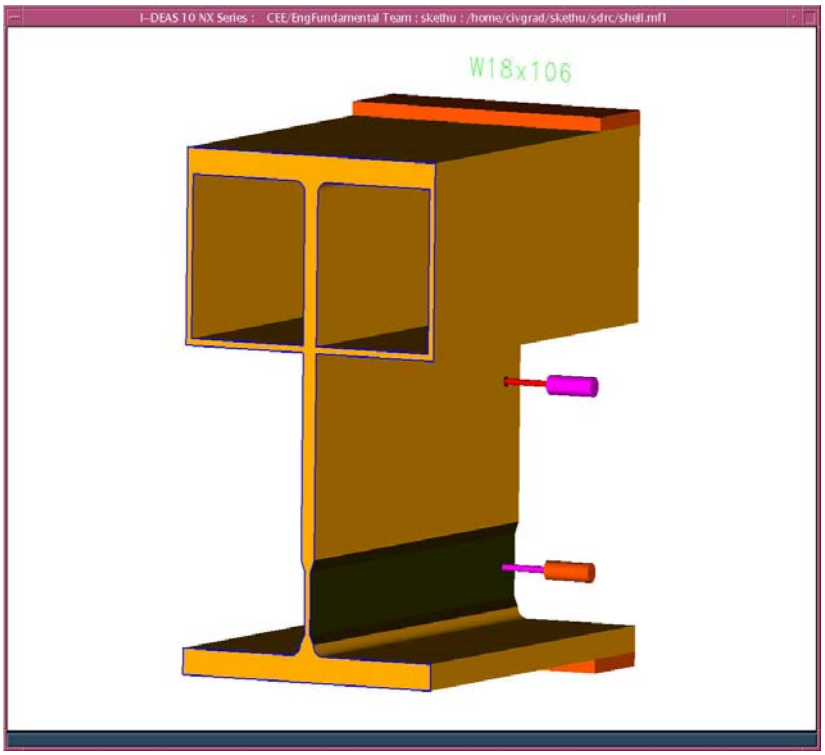

Figure 3.7 (a) I-DEAS model of the Experiment set up for specimen-1

Figure 3.7 (b) Experiment setup in the lab for specimen-1

3.4 Calculation of buckling/crushing load from experimental data

Recall that the purpose of the experiments was to confirm the accuracy of the finite element modeling procedure.

Specimen1

Figure 3.8 shows the load vs displacement graphs for the upper and lower LVDTs for specimen-1. The buckling load was not estimated from the load vs deflection graph because information on these phenomena is surprisingly limited. However, also identified within Figure 3.8 was the buckling/crushing capacity of 176 kips estimated using ABAQUS. Of course, it is very difficult to tell from the graph where the web begins to move laterally from the graph or even from the data itself, i.e. due to noise in the signal. However, it can be said with reasonable confidence that the buckling/crushing load prediction using ABAQUS easily falls within the margin of error associated with this type of comparison. In other words, the experiment confirms the adequacy of the numerical modeling procedure.

Interestingly, one might expect the experimental buckling load to be lower than the numerically predicted load due to imperfections, etc. This was not observed and was felt to be due to the fact that the 50 ksi steel specified may very likely have exceeded that yield strength, as well as the corresponding ultimate strength. The steel modeled in ABAQUS was 50 ksi steel and was undoubtedly weaker since specifying 50 ksi steel is a minimum. Also shown in Figure 3.8 is a photograph showing the specimen following testing. Beside it is the deformed IDEAS/ABAQUS model for comparison.

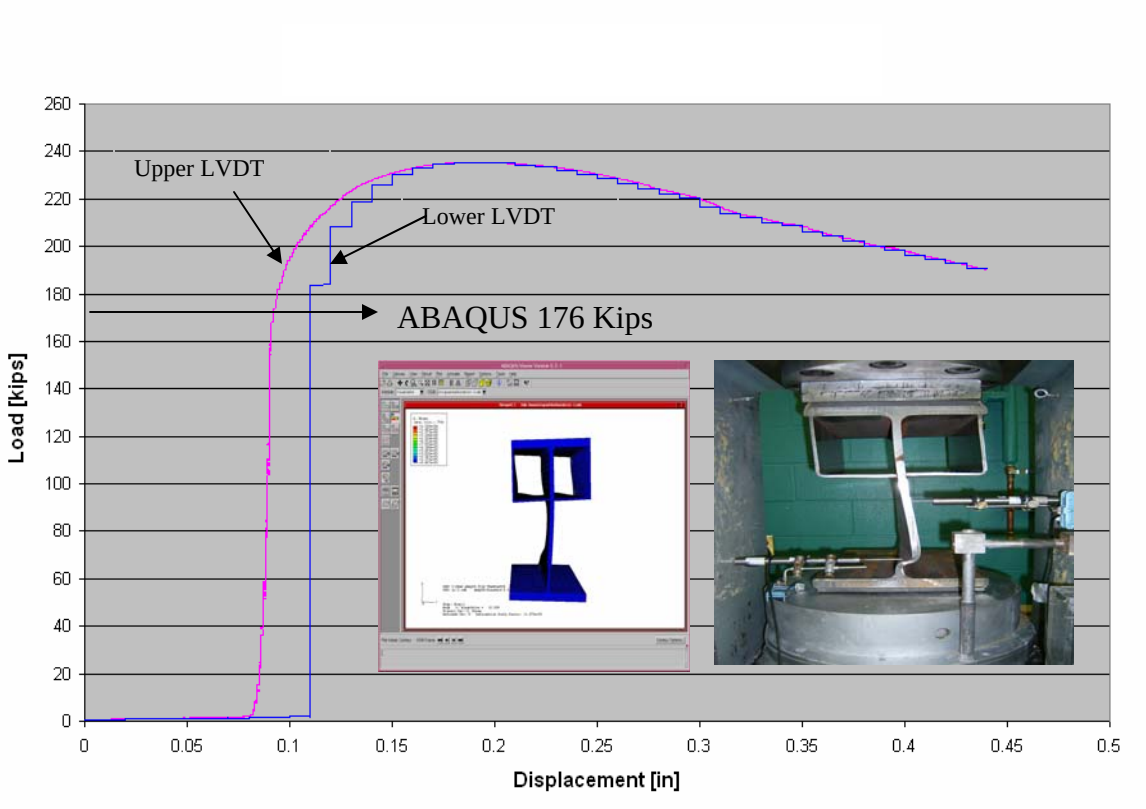

Figure 3.8 Load vs displacement curve for specimen-1

Specimen 2

Figure 3.9 shows the load vs displacement graphs for the upper and lower LVDTs mounted on specimen-2. The ABAQUS buckling /crushing load prediction for specimen-2 was 235 kips. It can be observed from the graph that the LVDTs start to deviate near this load. From plots in Figure 3.9 it can be seen that the ABAQUS deflection shape and deflection shape observed after testing specimen-2 provide a good match and the mode of buckling observed is mode 2.

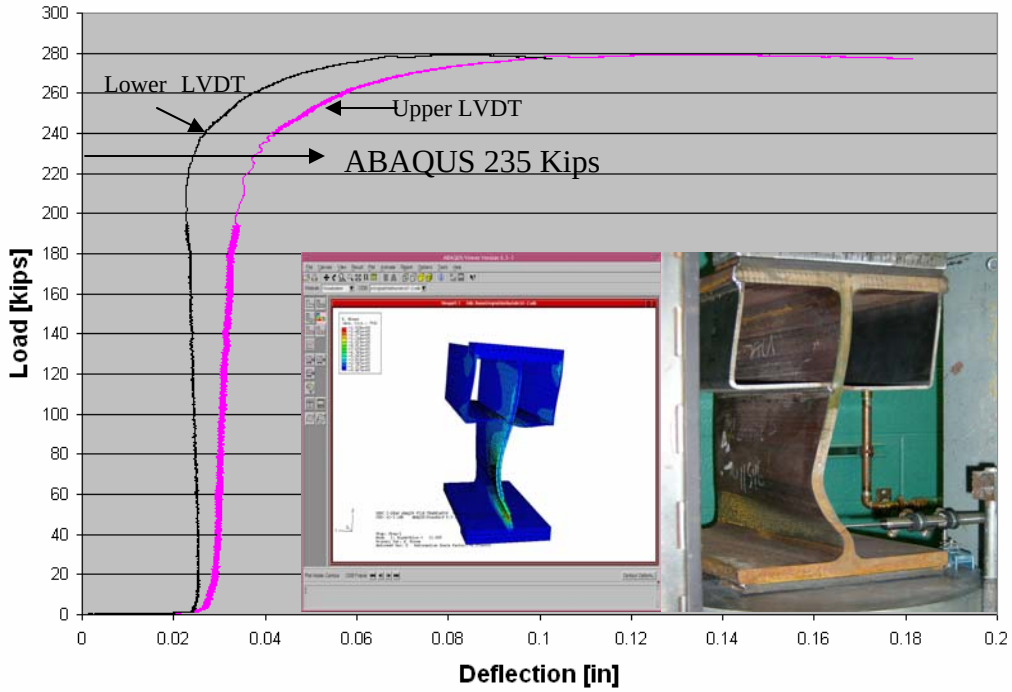

Figure 3.9 Load vs displacement curve for specimen-2

Specimen 3:

Figure 3.10 shows the load vs displacement graphs for upper and lower LVDTs mounted on specimen-3. The ABAQUS buckling/crushing load prediction for specimen-3 was 180 kips. The buckling shape predicted by the ABAQUS model appears to agree well with the experimental buckling shape, as seen by the figures superimposed on the graph. Some rotation at the top flange can be seen in the ABAQUS model. Recall the top flange was modeled as fixed. This did not appear to have a significant effect on the predicted capacity possibly because the horizontal ¼ inch plate (lateral bracing) carried a significant portion of the load as was planned.

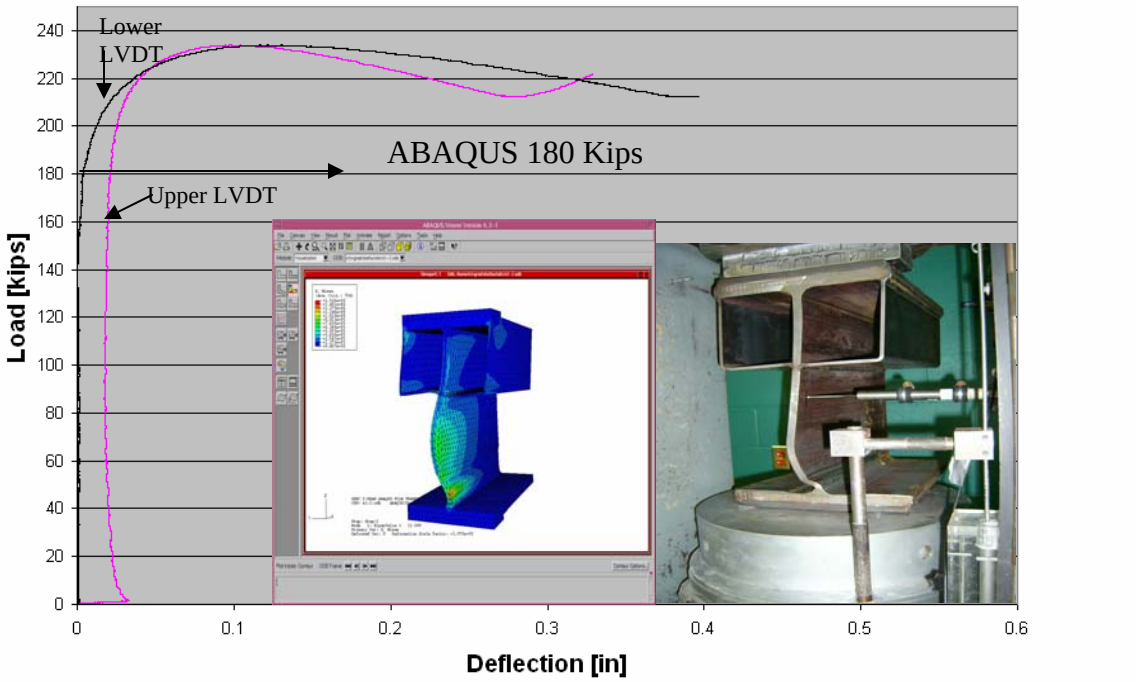

Figure 3.10 Load vs displacement curve for specimen-3

Specimen 4:

Figure 3.11 shows the load vs displacement graphs for upper and lower LVDTs mounted on specimen-4. The ABAQUS buckling /crushing load prediction for specimen-4 is 252 kips. As with the other graphs a photograph of the deformed shape and the ABAQUS model are shown.

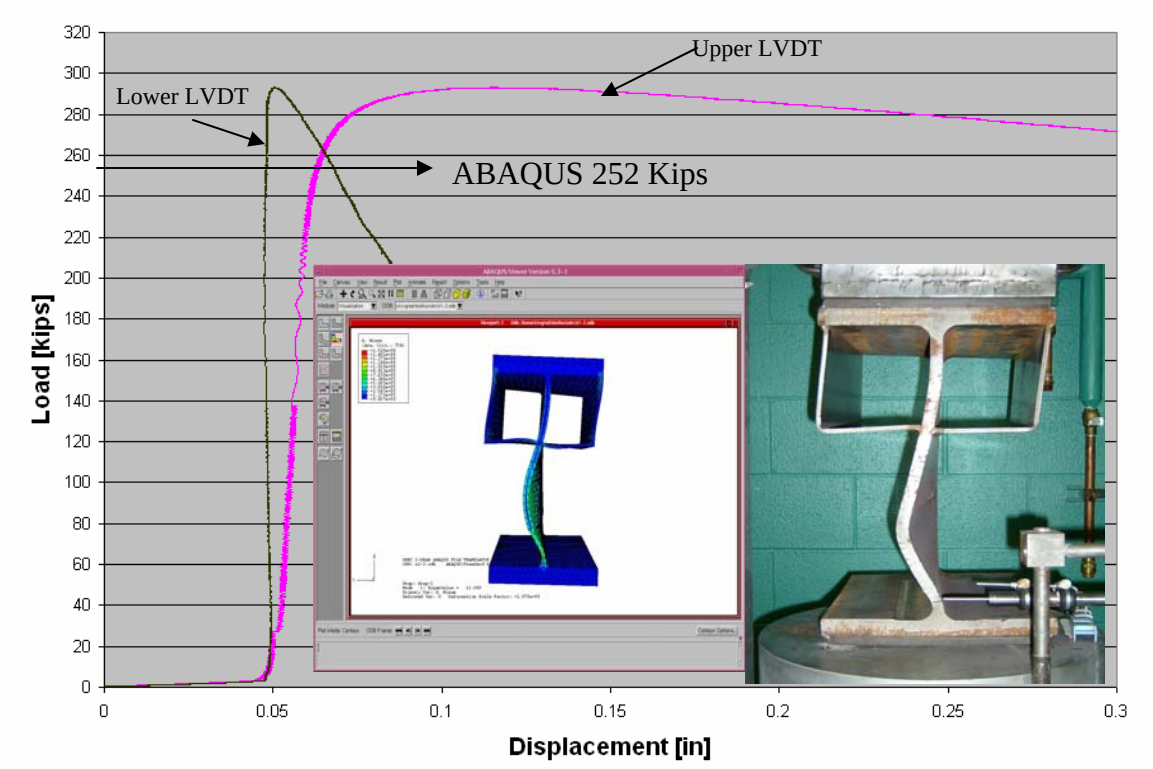

Figure 3.11 Load vs displacement curve for specimen-4

Based on the qualitative comparison of the numerically predicted buckling capacities with the experimental results, it can be concluded that the numerical model is an appropriate tool for use in the development of a simplified model.

4. DEVELOPMENT OF STRUCTURAL ANALYST DESIGN CHARTS

Recall that the primary objective of this study was to provide a quick, conservative technique for estimating the remaining capacity of a steel bridge beam end that is in early to intermediate stages of corrosive deterioration. No effort is made to investigate extremely severe cases since these do not require analysis, but simply repair and/or replacement. In an effort to demonstrate the effectiveness of the approach developed herein, the Michigan Department of Transportation's current approach is first explained. The new method is then developed and several comparisons made.

4.1 MDOT's current procedure

MDOT's current procedure consists of calculating the shear capacity, web crippling capacity, and web buckling capacity of a beam based on several simplifying assumptions. The minimum value of the above three quantities is taken as the governing capacity for the section. The following explains the procedure used to calculate the shear capacity, web crippling capacity, and web buckling capacity of a beam. The MDOT current procedure first calculates the reduced capacity by using equations from AISC (2002) based on the assumption that the whole web is deteriorated. Figure 4.1 shows MDOT's assumption. In the figure even though the web is corroded at the bottom (solid line), MDOT assumes that the whole web is corroded (dashed line).

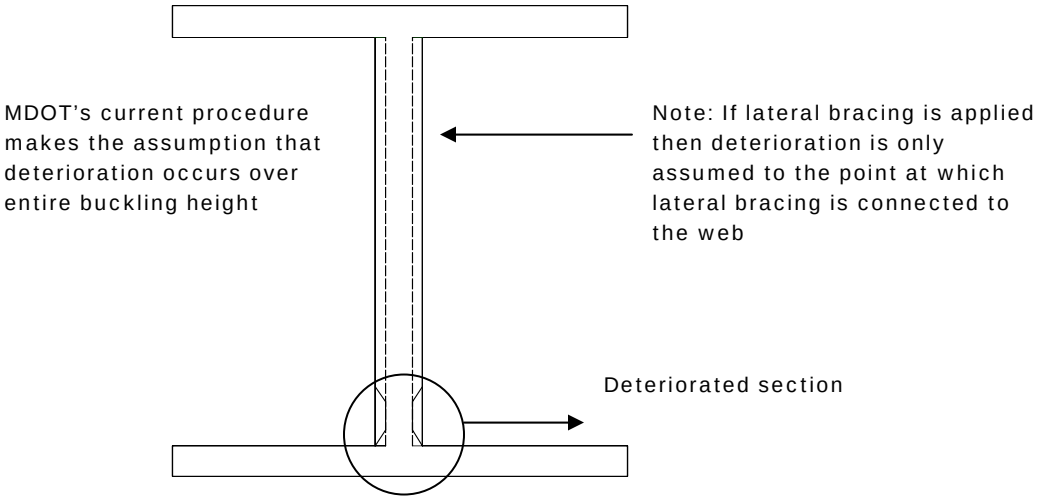

Figure 4.1 Picture showing MDOT's assumption in calculating the reduced capacity

4.1.1 Calculation of shear capacity

1. Total moment of inertia of the deteriorated I-section is calculated.

$$I = I_o + \sum A \times d^2 \tag{4.1}$$

where I is the total moment of inertia of the deteriorated section, I_o is the moment of inertia of the section calculated from the bottom flange, ΣAd^2 is the first moment of area about the bottom of flange.

2. Capacities at the top of the deteriorated web and at the centroid of the I-section are calculated by using the following formulae:

$$Q_1 = \sum A_1 \times d_1 \tag{4.2}$$

$$Q_2 = \sum A_2 \times d_2 \tag{4.3}$$

where Q_1 is the capacity at the top of deteriorated web, A_1 is the area above bottom flange up to the top of bad web, d_1 is the distance to the centroid of the area, A_2 is the area above bottom flange, and d_2 is the distance to the centroid of the area.

3. Allowable shear stress is

$$F_a = 0.45 \times F_y \tag{4.4}$$

where F_a is the allowable shear stress and F_y is the yield stress of the steel.

4. Shear capacity is

$$F_{shear} = \frac{F_a \times I \times t}{Q} \tag{4.5}$$

where F_{shear} is the shear capacity of the deteriorated section, t is the thickness of deteriorated web, Q is the smaller value of $Q1$ and $Q2$.

4.1.2 Calculation of web crippling capacity

1. Allowable stress for web crippling (F_{cr}) is calculated by using**:**

$$F_{cr} = 0.75 \times F_y \tag{4.6}$$

where F_y is the yield stress of the steel.

2. Effective length (L_{eff}) is calculated by using :

$$L_{eff} = N + k \tag{4.7}$$

where N is the bearing length and k is the fillet radius.

3. Capacity for web crippling (F_{crip}) is calculated by using the formula:

$$F_{crip} = F_{cr} \times t \times L_{eff} \tag{4.8}$$

where t is the thickness of the deteriorated portion of the web.

4.1.3 Calculation of web buckling capacity

1. The slenderness parameter (λ_c) is calculated by using the following formula:

$$\lambda_c = \frac{K \times L}{r} \tag{4.9}$$

where λ_c is slenderness parameter, K is a constant based on end boundary conditions, L is unbraced length, r is radius of gyration.

2. Column critical stress (F_{cr}) is calculated by using the LRFD Equations:

$$F_{cr} = (1 - \frac{\lambda_c^{\,2}}{4}) \times F_y \qquad \text{if } \lambda_c \leq 1.414 \tag{4.10}$$

$$F_{cr} = \frac{1}{\lambda_c^{\,2}} \times F_y \qquad \text{if } \lambda_c > 1.414 \tag{4.11}$$

3. Allowable axial compression stress F_a is given by:

$$F_a = \frac{F_{cr}}{FS} \tag{4.12}$$

where FS is factor of safety (FS=1.7).

4. Web buckling capacity is given by:

$$F_{buc} = F_a \times A_g \tag{4.13}$$

where A_g is the gross area (= $L_{eff} \times t$), L_{eff} is effective length = $18 \times t$; t is thickness of deteriorated portion of the web.

4.1.4 Governing capacity

The governing capacity of the beam then is given by:

$$\text{Capacity} = \min [F_{shear}, F_{crip}, F_{buc}] \quad (4.14)$$

In virtually all cases the buckling load is the minimum of all the three values (Kelley 2004). This was verified but not presented herein. So, as mentioned the Finite Element Analyses were performed to calculate the buckling loads for the beams in the bridge portfolio.

4.2 FEA results

FEA results consisted of buckling/crushing loads for the bridges in the bridge portfolio. Note that although there were sixteen bridges in the portfolio, some of the beams were the same. The results are divided into two parts namely results for damage on one side of the beam and results for damage on both sides of the beam.

Table 4.1 presents the results of the finite element analyses as a function of the damage height and damage depth for one-sided beam deterioration.

Table 4.2 has the same format as Table 4.1 except that it is for two sided deterioration. The difference in reduced buckling capacity was greater than two fold, although the section loss was only doubled. This was to be expected since the differential equation describing buckling is nonlinear.

Table 4.1 Remaining capacity for different beams damage on one side of the web from the bridge portfolio

Damage depth = 1/16"

	Remaining Capacity [%]					
Beam	Damage height					
	0"	0.5"	1.5"	3"	5"	9"
W36x260	100	99	98	95	94	89
W36x230	100	97	96	94	92	88
W33x152	100	98	96	94	91	87
W33x141	100	98	96	93	90	86
W30x116	100	98	95	90	87	83
W30x108	100	97	96	92	89	85
W27x84	100	97	93	88	85	81
Mean	100	98	96	92	90	85
Standard deviation	0.00	0.76	1.50	2.50	3.04	2.82

Damage depth = 1/8"

	Remaining Capacity [%]					
Beam	Damage height					
	0"	0.5"	1.5"	3"	5"	9"
W36x260	100	98	95	90	87	79
W36x230	100	97	94	89	85	79
W33x152	100	97	90	86	82	76
W33x141	100	96	92	84	80	70
W30x116	100	95	90	87	81	75
W30x108	100	96	91	83	77	72
W27x84	100	93	85	76	71	68
Mean	100	96	91	85	80	74
Standard deviation	0.00	1.63	3.27	4.69	5.29	4.30

Damage depth = 3/16"

	Remaining Capacity [%]					
Beam	Damage height					
	0"	0.5"	1.5"	3"	5"	9"
W36x260	100	97	92	86	79	69
W36x230	100	92	91	79	76	70
W33x152	100	96	88	77	70	65
W33x141	100	94	86	75	67	61
W30x116	100	92	87	79	75	67
W30x108	100	93	84	72	65	57
W27x84	100	90	75	64	61	56
Mean	100	93	86	76	71	64
Standard deviation	0.00	2.44	5.64	6.83	6.53	5.65

Table 4.2 Remaining capacity for different beams for damage on both sides of the web from the bridge portfolio

Damage depth = 1/16"

	Remaining Capacity [%]					
Beam	Damage height					
	0"	0.5"	1.5"	3"	5"	9"
W36x260	100	95	92	88	85	80
W36x230	100	94	90	86	82	77
W33x152	100	93	89	84	79	73
W33x141	100	93	88	83	77	71
W30x116	100	94	89	84	78	71
W30x108	100	92	87	80	75	69
W27x84	100	89	81	74	66	61
Mean	100	93	88	83	77	72
Standard deviation	0.00	1.95	3.46	4.57	6.02	6.07

Damage depth = 1/8"

	Remaining Capacity [%]					
Beam	Damage height					
	0"	0.5"	1.5"	3"	5"	9"
W36x260	100	90	83	76	69	62
W36x230	100	89	80	71	64	57
W33x152	100	85	73	63	56	50
W33x141	100	84	72	61	51	46
W30x116	100	83	70	59	51	45
W30x108	100	80	67	56	48	43
W27x84	100	69	51	42	36	31
Mean	100	83	71	61	53	48
Standard deviation	0.00	7.01	10.38	10.95	10.85	10.06

Damage depth = 3/16"

	Remaining Capacity [%]					
Beam	Damage height					
	0"	0.5"	1.5"	3"	5"	9"
W36x260	100	80	69	59	44	34
W36x230	100	75	62	56	47	36
W33x152	100	63	48	39	33	27
W33x141	100	61	43	36	30	24
W30x116	100	54	38	32	25	22
W30x108	100	51	35	29	24	19
W27x84	100	50	36	30	24	20
Mean	100	59	44	38	30	24
Standard deviation	0.00	11.72	13.36	12.38	9.57	6.71

4.3 Deterioration factor (Ψ_d)

In order to provide structural analysts with a simplified approach for calculating the buckling/crushing capacity of a beam, a deterioration factor, Ψ_d , was defined as the ratio of the reduced capacity to the undamaged capacity. This was possible primarily because this study was confined to rolled sections with similar depths. The reduced capacity of the beam ($F_{reduced}$) due to deterioration determined using FE Analysis is calculated by multiplying the undamaged capacity ($F_{undamaged}$) of the original beam by the deterioration factor (Ψ_d). It can be written mathematically as

$$F_{reduced} = \Psi_d \times F_{undamaged} \tag{4.15}$$

4.4 Design charts

The design charts were developed in an effort to allow one to directly read the deterioration factor, $\Psi_{d,}$ for a given damage depth and damage height for a beam. The design charts were developed for two-sided damage and one-sided damage. They use a height ratio defined as the ratio of damage height to the unbraced web height on the abscissa and deterioration factor on the ordinate for different damage depths as shown in Figure 4.1.

The solid bold line shows the mean value of the deterioration factor as a function of the height ratio. The upper and lower dashed lines represents mean plus and minus 1.5 times the standard deviation, respectively. The lower line is the “design line”, i.e. it will be the one used in equation 4.15 to estimate the remaining capacity of a section. It should be noted that the minus one and half standard deviation was selected arbitrarily, but was felt to be significantly conservative. An example of the use of the design charts is presented in a later section.

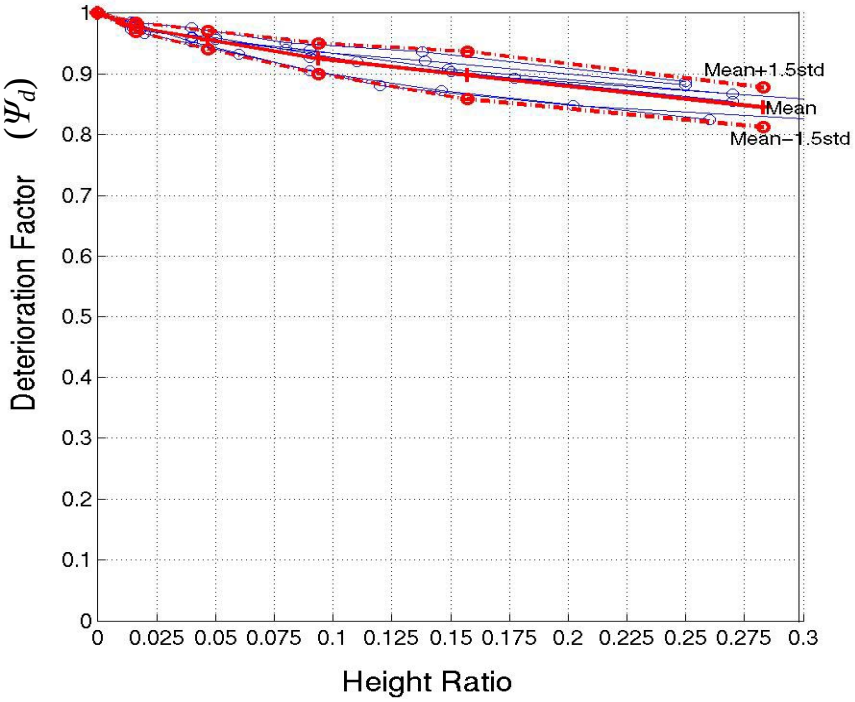

Figure 4.2 Deterioration factor vs height ratio for 1/16” one-sided damage

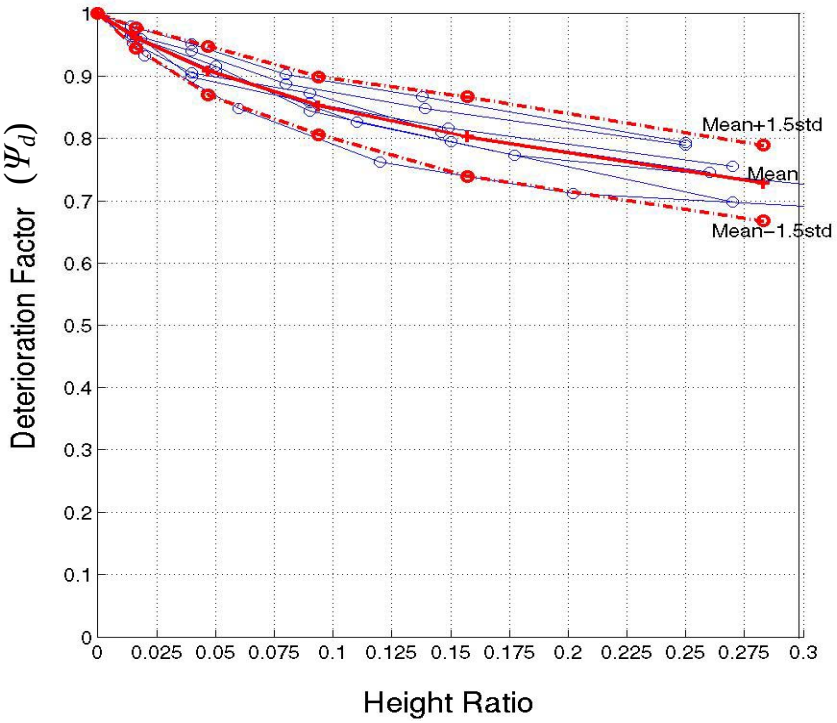

Figure 4.3 Deterioration factor vs height ratio for 1/8” one-sided damage

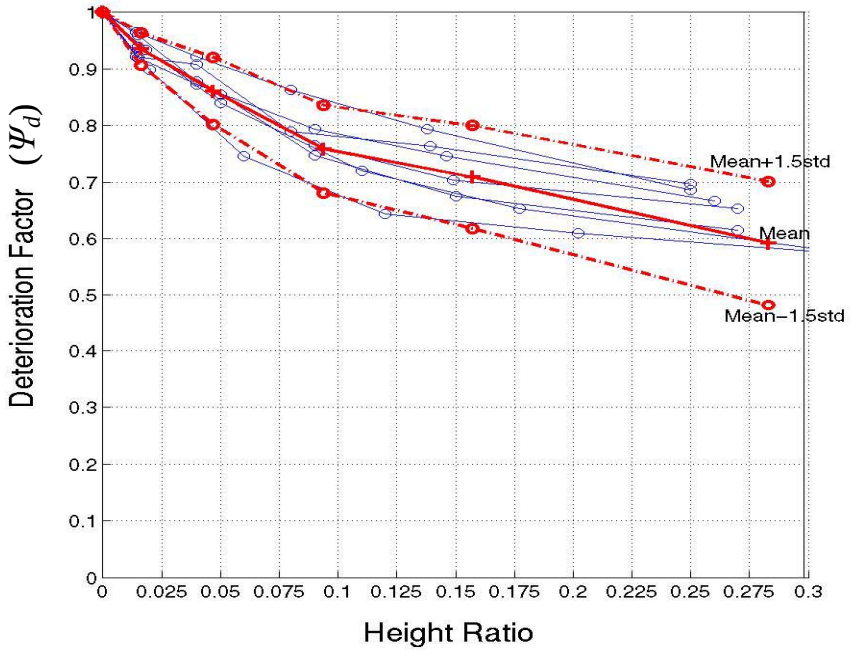

Figure 4.4 Deterioration factor vs height ratio for 3/16" one-sided damage

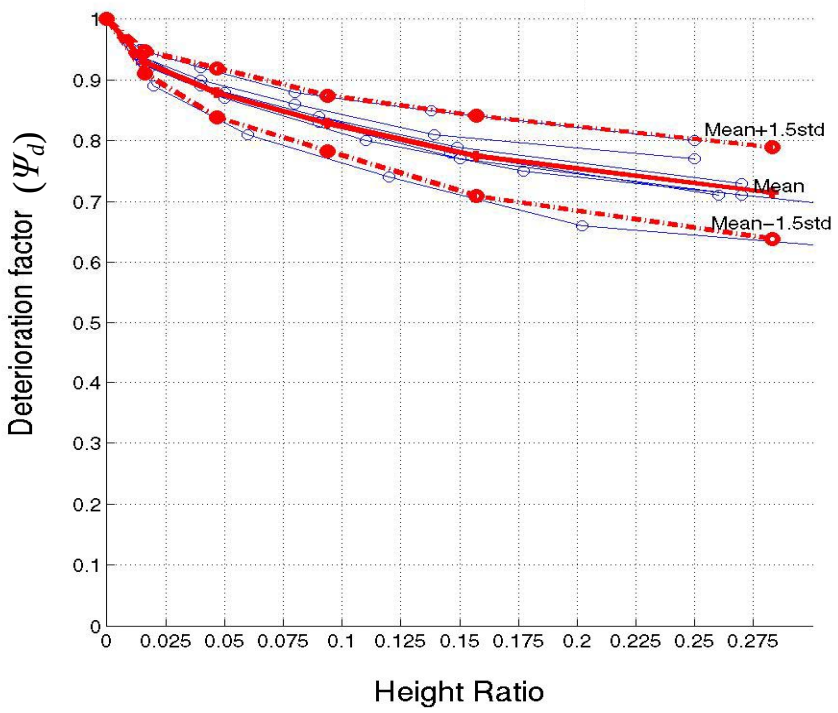

Figure 4.5 Deterioration factor vs height ratio for 1/16" two-sided damage

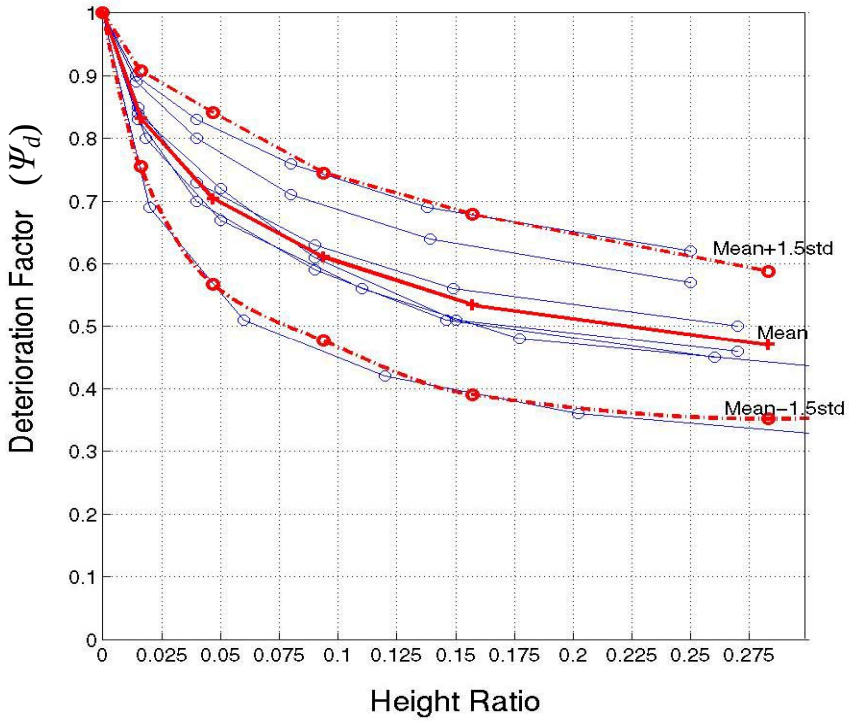

Figure 4.6 Deterioration factor vs height ratio for 1/8" two-sided damage

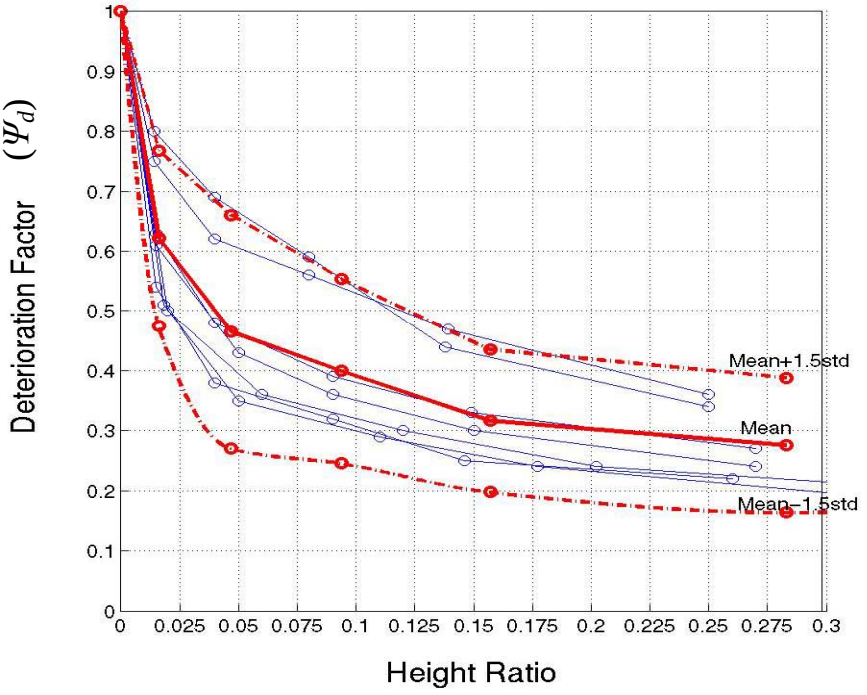

Figure 4.7 Deterioration factor vs height ratio for 3/16" for two-sided damage

Now, by taking each of the minus one and a half standard deviation lines from the plots presented and placing them on a single graph, we obtain the design chart. The 1.5 standard deviation was used because the use of charts is limited to rolled beams with depths between 27 inches and 36 inches. And also the model is assumed as fixed at the bottom and pinned at the top which is conservative. The 1.5 standard deviation also covers the data of all the beams. Figure 4.7 and Figure 4.8 show the one-sided design chart and two-sided design chart, respectively.

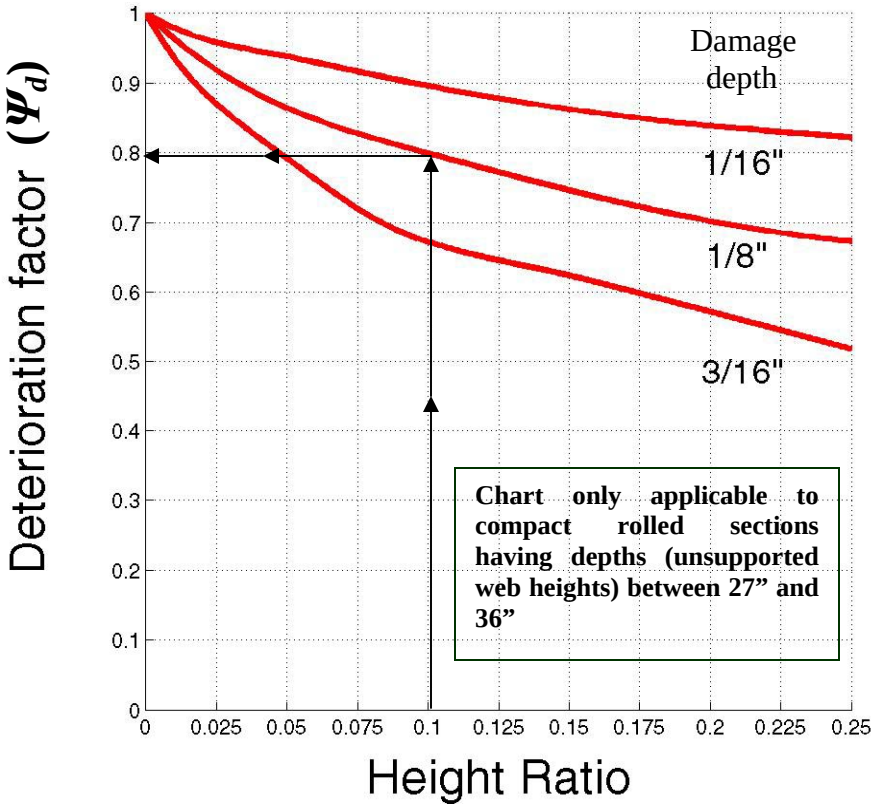

Figure 4.7 Design chart for damage on one side of the web

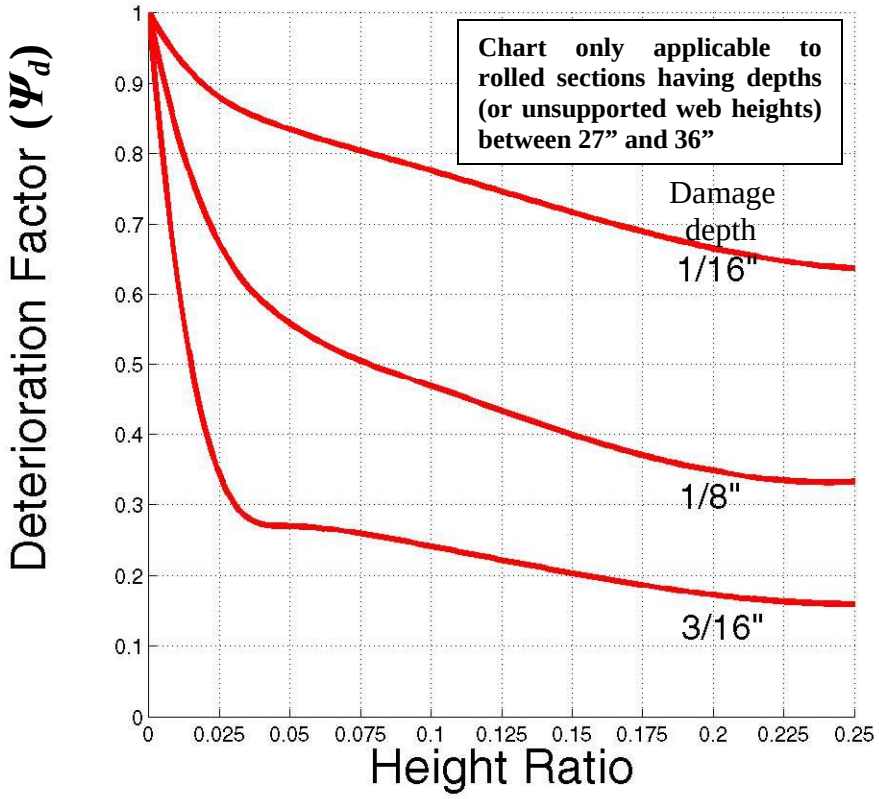

Figure 4.8 Design chart for damage on both sides of the web

4.5 Procedure to find the reduced capacity using design charts

Step 1

Determine if the damage is located on one side or both sides of the web. Conservatively determine damage depth.

Step 2

Determine the damage height in a conservative manner, i.e. select the highest points of damage located vertically above one another. If there is a doubt, be sure to over estimate the height.

Step 3

Determine the height of the unbraced web. If there is no lateral bracing, this should be taken as the beam depth. If there is lateral bracing, this should be taken as the distance between the bottom of the beam to the lateral bracing.

Step 4

Compute the height ratio as

$$\text{height ratio} = \frac{\text{Damage height from step 2}}{\text{Unbraced web height from step 3}} \tag{4.16}$$

Step 5

Find the height ratio calculated in step 4 on x-axis of either Figure 4.7 or Figure 4.8 (i.e., one-sided or two-sided damage). Move vertically up to the appropriate damage depth (use linear interpolation as necessary) and move left to the ordinate of the chart. The intersection with the ordinate indicates the deterioration factor, Ψ_d, to be used in equation 4.15. The arrows in Figure 4.7 indicate the procedure.

Step 6

Compute the reduced capacity ($F_{reduced}$) from equation 4.15 by multiplying the undamaged capacity ($F_{undamaged}$) of the original beam by the deterioration factor (Ψ_d).

$$F_{reduced} = \Psi_d \times F_{undamaged}$$

4.6 Determination of Deterioration Factor - Worksheet

General information:
Bridge #: _____
Beam end location: _____
Date of inspection: _____
Date of analysis: _____

(1) Is the damage located on <u>one</u> or <u>both</u> sides of the web?

Damage depth = _____

(2) Damage height =_____
(Select the highest point of damage located vertically)

(3) Height of the unbraced web =_____
- not laterally braced: height taken as the beam depth.
- laterally braced: height taken as the distance between the bottom of the beam to lateral bracing.

(4) Height ratio = $\frac{\text{Damage height (2)}}{\text{Unbraced web height (3)}}$ = _____

(5) Use appropriate figure below in determination of the deterioration factor.

Deterioration factor =_____

(6) Compute the reduced capacity using the above found deterioration factor.

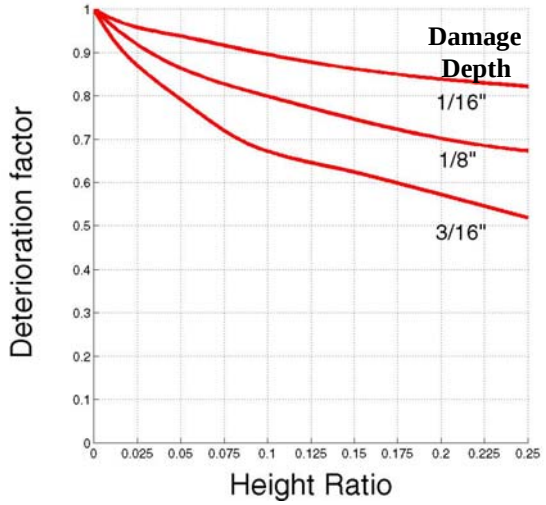

Design Chart for damage on one side of web.

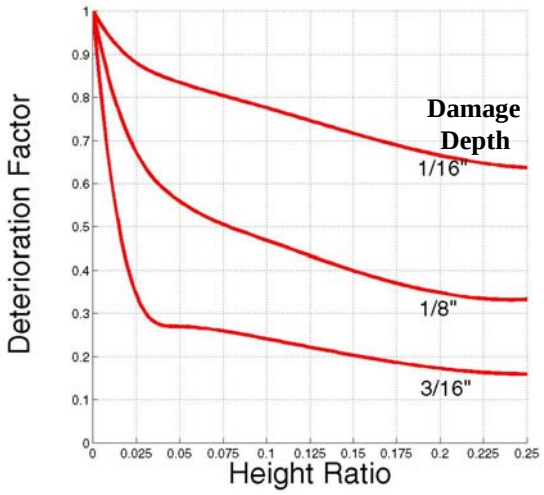

Design chart for damage on both sides of web.

4.7 Determination of Deterioration Factor - Example

From MDOT detailed beam survey report:

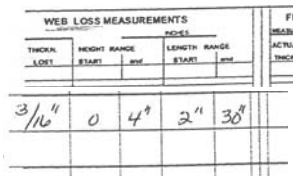

Givens: Bridge #: __123-xyz__
Beam end location: _Span 1S Beam 9W_
Date of inspection: __6/1/2004__
Date of analysis: __9/25/2004__
Height of the unbraced web: ____36”____
Damage is on one side of the web.

(6) Is the damage located on one or both sides of the web?

Damage depth = __3/16”__

(7) Damage height =___4”___
(Select the highest point of damage located vertically)

(8) Height of the unbraced web =___36”___
- not laterally braced: height taken as the beam depth.
- laterally braced: height taken as the distance between the bottom of the beam to lateral bracing.

(9) Height ratio =___Damage height (2)___ = _4/36 → 0.11_
Unbraced web height (3)

(10) Use appropriate figure below in determination of the deterioration factor.

Deterioration factor =___0.66___

(6) Compute the reduced capacity using the above found deterioration factor.

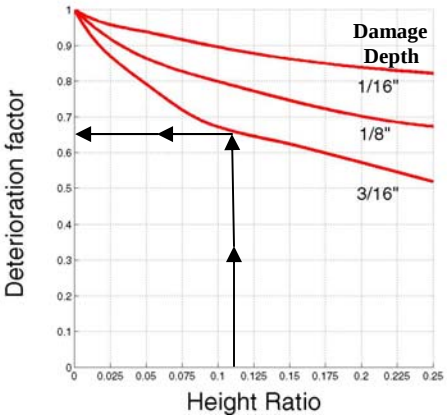

Design Chart for damage on one side of web.

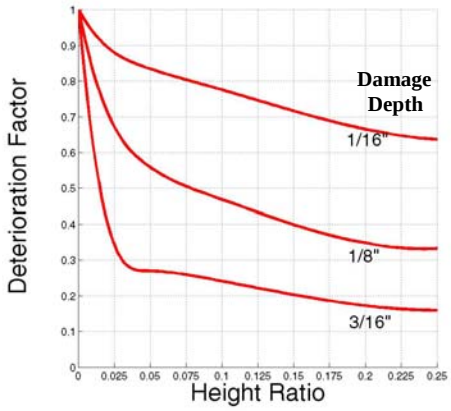

Design chart for damage on both sides of web.

4.5 Comparison of deterioration factor method (DFM) results to MDOT's current practice

In order to compare the deterioration factor method (DFM) developed herein with results using MDOT's current practice, a beam was selected from the bridge portfolio for analysis. The reduced capacity of the beam was calculated by using the MDOT method from a mathcad program provided by R. Kelley (2004) of MDOT. The reduced capacity of the same beam with the same deterioration was calculated from the design charts developed presented in Figure 4.7 and Figure 4.8. Table 4.3 shows the comparison between DFM results and MDOT results. The results shown in Table 4.3 provide some insight into the conservativeness of the DFM as well as some over-simplification observed in the current MDOT procedure.

Table 4.3 Comparison between DFM results and MDOT's current practice results

No of sides	Depth [in]	Height [in]	Buckling / Crushing capacity [kips]		% Difference
			Current MDOT	DFM method	
1	0.0625	1.5	140	160	12
1	0.0625	3	140	151	7
1	0.0625	5	140	146	4
1	0.0625	9	140	139	-1
1	0.125	1.5	114	148	23
1	0.125	3	114	136	16
1	0.125	5	114	128	11
1	0.125	9	114	116	2
2	0.0625	1.5	114	143	20
2	0.0625	3	114	133	14
2	0.0625	5	114	121	6
2	0.0625	9	114	114	0
2	0.125	1.5	72	101	29
2	0.125	3	72	84	14
2	0.125	5	72	72.2	0
2	0.125	9	72	63.8	-13

5. SUMMARY, CONCUSIONS AND RECOMMENDATIONS

5.1 Summary

The primary objective of this study was to provide structural analysts a simplified, quick, and accurate method for determining the reduced capacity of corrosively deteriorated steel beam bridges. The finite element packages SDRC I-DEAS and ABAQUS were used to model the steel beams in this study. Numerical simulations were performed on steel beams selected from a bridge portfolio of sixteen bridges. These beam sizes were fairly typical MDOT rolled sections used throughout the state. The validated finite element results were checked through a small experimental test program at Michigan Technological University.

The results from numerical simulations were used to develop the design charts that provided a conservative estimate of the remaining capacity of a deteriorated beam, assuming buckling controlled the design. A so-called deterioration factor can be identified from the design charts for different damage depths and damage heights. The reduced capacity can be calculated by multiplying the original capacity by the deterioration factor. The deterioration factor method is compared with the MDOT method which uses AISC equations to calculate the reduced capacity assuming the entire web (or unbraced height) is deteriorated.

5.2 Conclusions

Based on the material presented herein the following conclusions were reached.

1. The finite element models developed were capable of modeling and thus predicting the buckling/crushing loads for typical rolled beams. The difference between the results from FEA results and experimental results, although not precisely determined, was acceptable.
2. The accuracy of the deterioration factor method (DFM) developed is approximately the same as the MDOT method.

3. The DFM is able to provide a rapid estimate of the remaining buckling capacity of a bridge beam for MDOT.

5.3 Recommendations

As with all research projects, there was a finite amount of work that could be completed within the scope of this project.

1. This study was limited to rolled sections only. Extension of this study to plate girders with bearing stiffeners should be pursued.
2. In the present study the composite behavior of the concrete slab steel bridge is not considered. It was assumed that the wheel load is transferred to the steel beam without any slippage. Full analyses of the composite deck girder bridges are recommended.
3. In this study the buckling/crushing capacity of the beams was considered because it was found from the MDOT calculations that buckling/crushing load governs the capacity in a very high percentage of the cases. A detailed analysis of shear capacity as well as bearing capacity is recommended, analogous approach for those load effects/failure mechanisms will provide the completeness necessary to comprehensively solve this problem.

6. REFERENCES

American Association of State Highway and Transportation Officials. *Bridge Design Specifications – Load and Resistance Factor Design*, 2nd edition. Washington D.C. AASHTO, 2002 Interim.

American Institute of Steel Construction. *Manual of Steel Construction Load and Resistance Factor Design*, 3rd edition. Chicago, Illiniois: AISC, 2000.

Kayser, J.R. and A.S. Nowak.(1989), "Capacity Loss Due to Corrosion in Steel-Girder Bridges", *ASCE Journal of Structural Engineering*, Vol. 115, No. 6, June 1989, pp. 1525-1537.

Kemp, A.R.(1996), "Inelastic Local and Lateral Buckling in Design Codes", *ASCE Journal of Structural Engineering*,. Vol. 122, No. 4, April 1996, pp. 374-382.

Kelley, R (2004) *Personal communication.*

Kulicki J.M., Z.Prucz, D.F.Sorgenfrei, and D.R.Mertz. "Guidelines for Evaluating Corrosion Effects In Existing Steel Bridges", *National Cooperative Highway Research Program Report* 333, NCHRP 1990.

7. APPENDIX A

Notations

A_o - original cross sectional area

A_d - reduced cross sectional area

q - Loss coefficient

RCF_l - local residual capacity factor

RCF_m – member residual capacity factor

C_m – capacity of the original member

C_{dm} – capacity of the damaged member

C – average corrosion penetration in microns

n – number of years

a and b – parameters determined from regression analysis of experimental data

$[k_o]$ – initial stiffness matrix

λ_i – eigenvalue of the i^{th} mode

$[k_d]$ – stiffness matrix due to incremental loading

V_i – eigenvectors

D_d – damage depth

D_h - damage height

D_{fw} – flange damage width

D_{ww} – web damage width

I – total moment of inertia of the deteriorated section

I_o – moment of inertia of the section calculated from bottom flange

ΣAd^2 – first moment of area about bottom of flange

Q_1 - capacity at the top of deteriorated web

Q_2 – capacity at the centroid of the section

A_1 - area above bottom flange up to the top of bad web

A_2 - area above bottom flange

d_1 - distance to the centroid of the area,

d_2 - distance to the centroid of the area.

F_a – allowable shear stress

F_y – yield stress of steel

F_{shear} – shear capacity of deteriorated section

F_{cr} – allowable stress for crippling

F_{crip} – capacity for web crippling

t – thickness of deteriorated web

L_{eff} - effective length

N – bearing length

K – fillet radius

L – unbraced length

r – radius of gyration

λ_c- slenderness parameter

F_{buc} – web buckling capacity

FS – factor of safety

A_g – gross area

$F_{reduced}$ – reduced capacity of the beam

$F_{undamaged}$ – undamaged capacity of the beam

Ψ_d – deterioration factor

8. APPENDIX B

This section presents the procedure employed to create, analyze and view the results of the finite element model used in this study. A W36x230 beam was selected from the bridge portfolio for this purpose. The load was applied in increments of 3 kips. The objective is to determine the buckling load. The following steps show the procedure.

Step 1

Create the model by using **Simulation>Master modeler** in SDRC IDEAS. The following screen shot shows the model created in IDEAS.

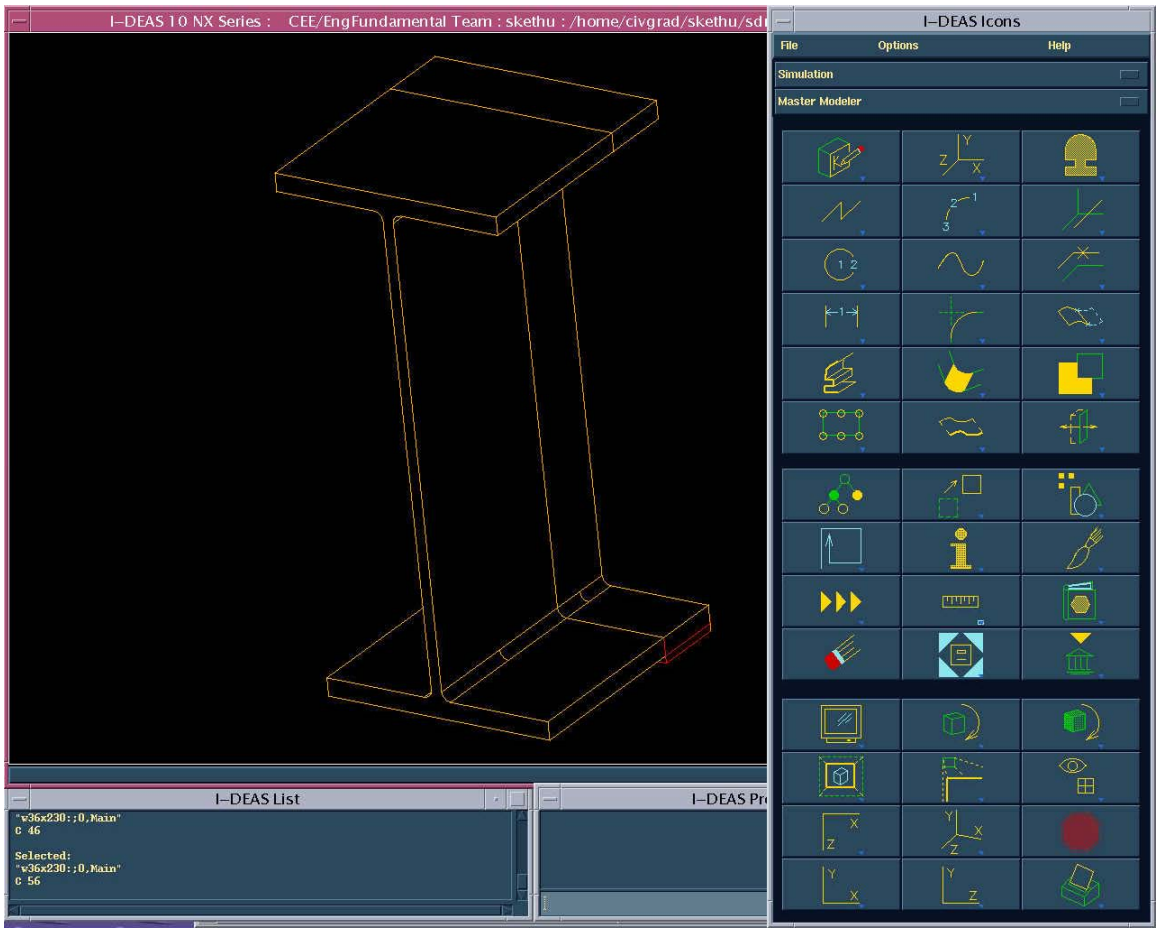

Step 2

Mesh the model using **Simulation>Meshing** in IDEAS. The following screen shots show the meshed model. Define the material properties for steel in the meshing module.

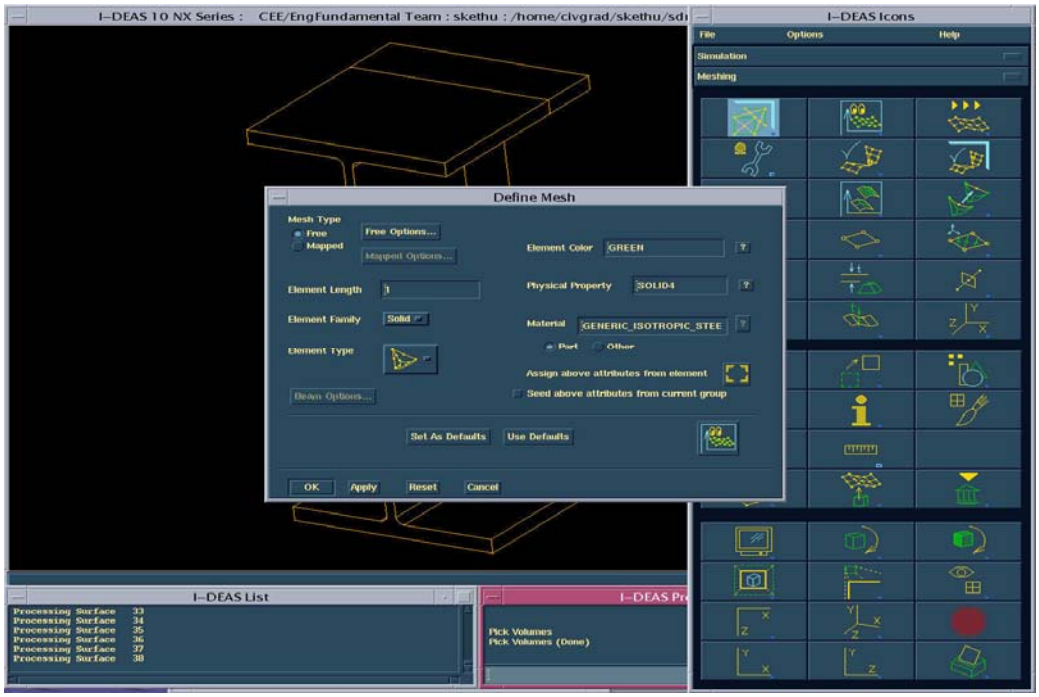

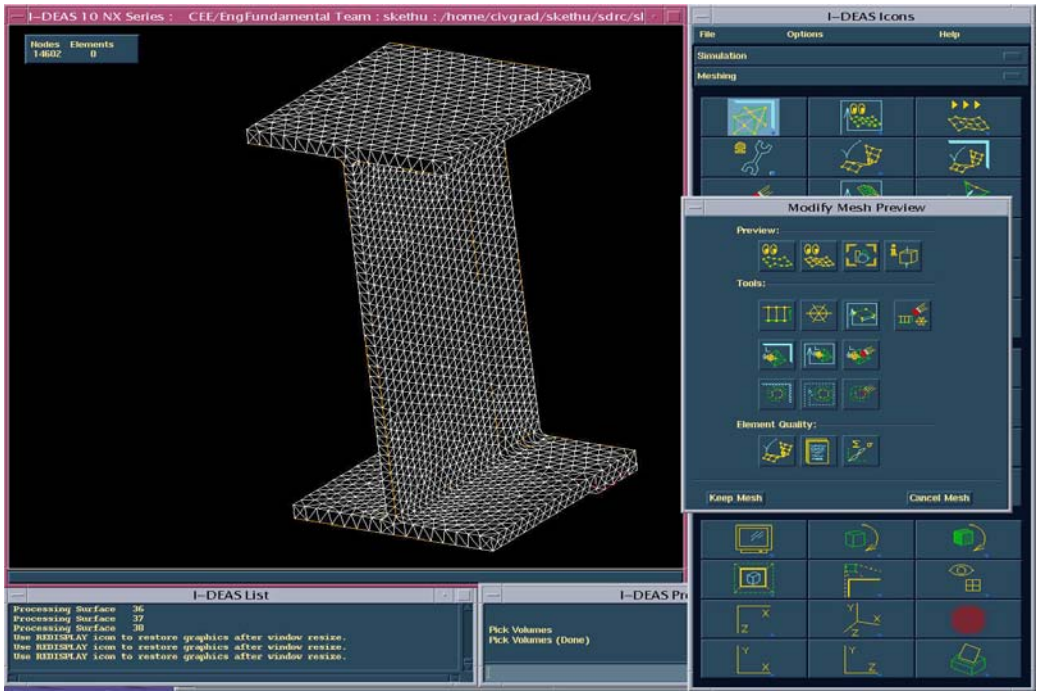

Step 3

Apply the boundary conditions by using the module **Simulation>boundary conditions**. The model after applying boundary conditions is shown below.

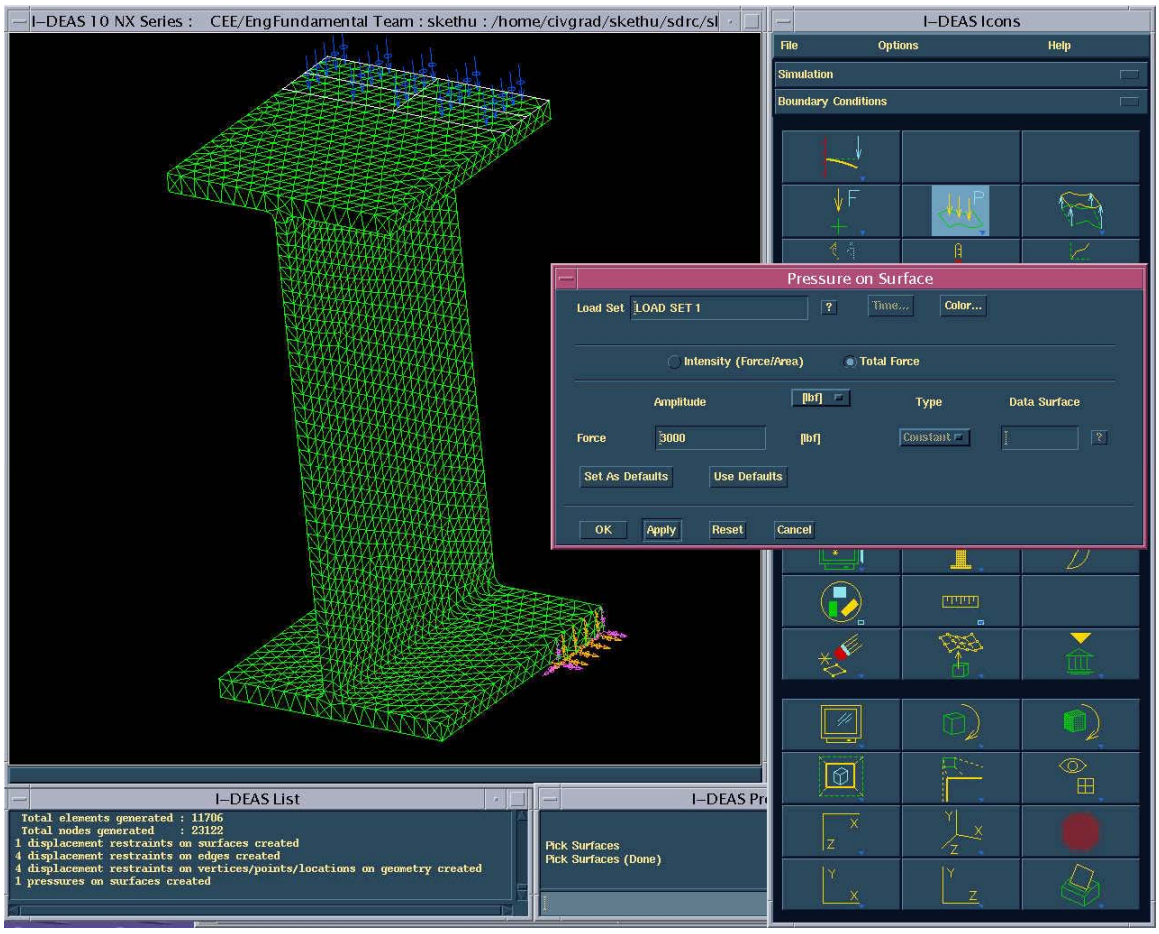

Step 4

Export the model to ABAQUS by creating an input file for ABAQUS solver using **File>export** in IDEAS. Choose the buckle option for the analysis type while creating the input file for ABAQUS. Give a valid filename to the input file.

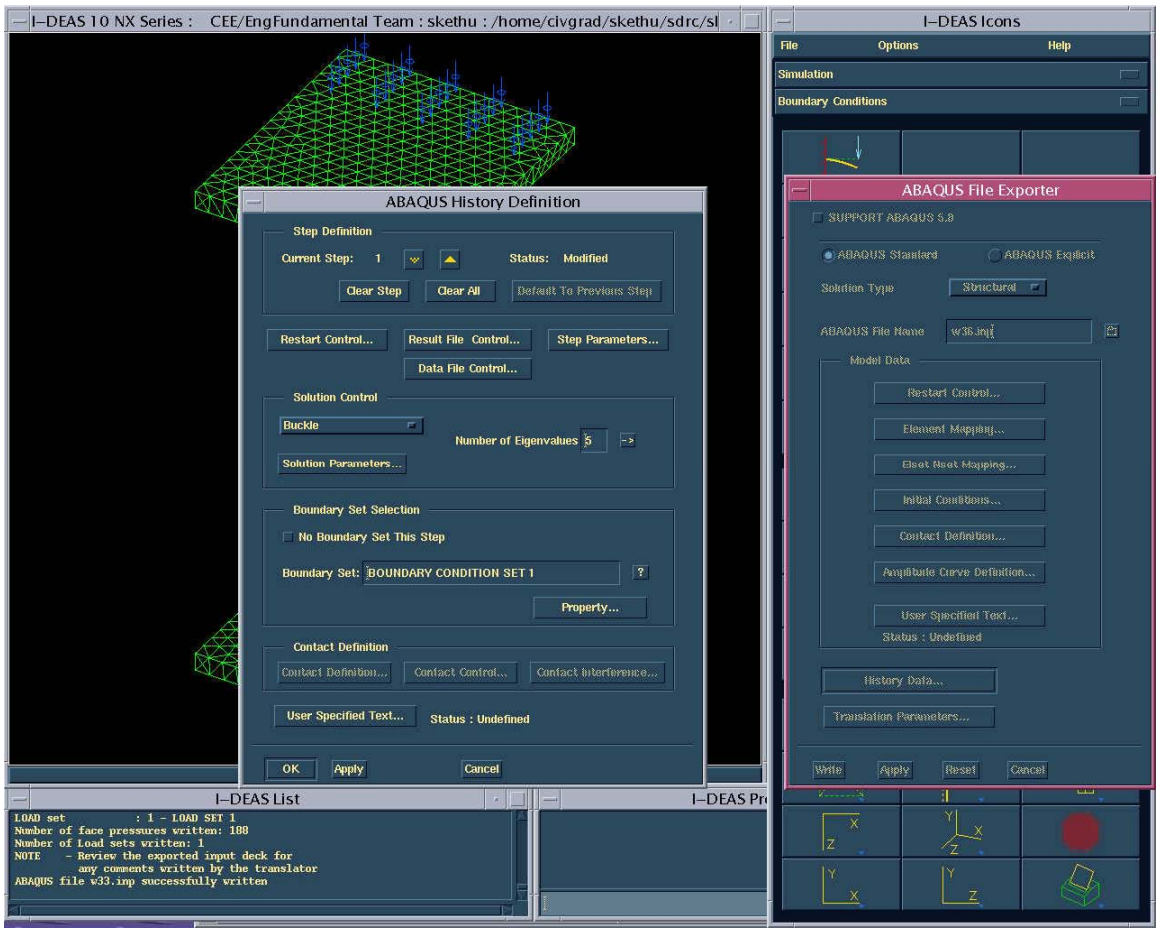

Step 5

Open an xterm window and type the command (abaqus job=’filename.inp’ int).

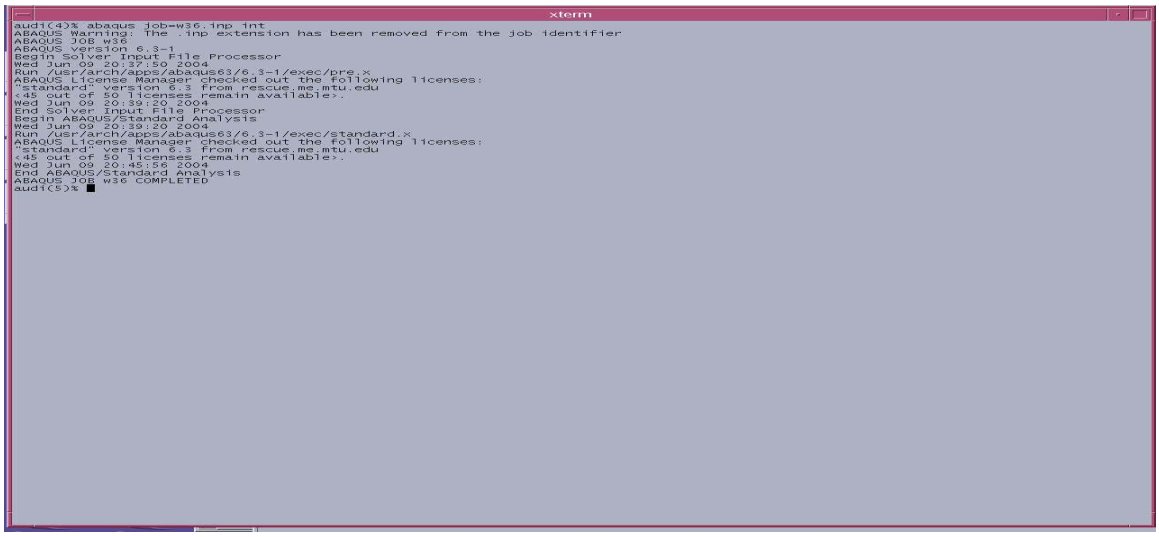

Step 6

View the results by opening the ABAQUS viewer window. The buckling load is calculated by multiplying the applied load by the lowest eigenvalue obtained from ABAQUS. The following picture shows the ABAQUS viewer screen shot.